This is to certify that the

dissertation entitled

TIME-RESOLVED RESONANCE RAMAN DETECTION OF INTERMEDIATES IN THE REDUCTION OF DIOXYGEN BY CYTOCHROME OXIDASE

presented by

CONSTANTINOS A. VAROTSIS

has been accepted towards fulfillment
of the requirements for

Ph.D degree in CHEMICAL PHYSICS

Gerald T. Babcock
Major professor

Date June 18, 1990

TIME-RESOLVED RESONANCE RAMAN DETECTION OF INTERMEDIATES IN THE REDUCTION OF DIOXYGEN BY CYTOCHROME OXIDASE

By

Constantinos A. Varotsis

A DISSERTATION

Submitted to

Michigan State University
in partial fulfillment of the requirements
for the degree of

DOCTOR OF PHILOSOPHY

Chemical Physics Program

1990

ABSTRACT

TIME-RESOLVED RESONANCE RAMAN DETECTION OF INTERMEDIATES IN THE REDUCTION OF DIOXYGEN BY CYTOCHROME OXIDASE

By

Constantinos A. Varotsis

Cytochrome oxidase, also known as cytochrome aa_3, the terminal enzyme of the mitochondrial respiratory chain, catalyzes the reduction of molecular oxygen to water. In the work reported here, we used a combination of rapid mixing, laser photolysis, and a novel jet apparatus that produces a continuous stream of sample in air to detect the transient intermediates formed in the reactions of fully-reduced and mixed-valence cytochrome oxidase with dioxygen. In the spectrum recorded at 10 μs subsequent to carbon-monoxide photolysis of the fully-reduced enzyme in the presence of O_2, a mode is observed at 571 cm^{-1} that shifts to 546 cm^{-1} when the experiment is repeated with $^{18}O_2$. The appearance of this mode is dependent upon the laser intensity used and disappears at higher-incident energies. The high-frequency data, in conjunction with the mid-frequency data, allow us to assign the 571 cm^{-1} mode to the Fe-O stretching vibration of the low-spin O_2 adduct that forms in the fully-reduced cytochrome oxidase/dioxygen reaction. The 571 cm^{-1} $\nu(Fe-O_2)$ frequency in the fully-

reduced enzyme/O_2 adduct is essentially identical to the 572 cm^{-1} frequency we measured for this mode during thereduction of O_2 by the mixed-valence enzyme, which indicates that the O_2-bound cytochrome a_3 is independent of the redox state of the cytochrome a/Cu_A pair. In the spectrum recorded at 800 μs in the reaction of the fully-reduced enzyme with O_2, a mode is observed at 790 cm^{-1} that shifts to 755 cm^{-1} when the experiment is repeated with $^{18}O_2$. The frequency of this vibration and the magnitude of the $^{18}O_2$ isotopic frequency shift allow us to assign the 790 cm^{-1} mode to the Fe^{IV}=O stretching vibration of the $a^{3+}a_3{}^{IV}$=O/$Cu_B{}^{1+}$ adduct that forms in the fully-reduced cytochrome oxidase. The appearance of this mode is not affected when D_2O was used as a solvent. This suggests that the ferryl-oxo intermediate is not hydrogen-bonded. The high-frequency (1000-1700 cm^{-1}) Raman data during the oxidase/O_2 reaction show that the oxidation of cytochrome a^{2+} is biphasic. The faster phase is completed in 100 μs and is followed by a plateau region in which no further oxidation of cytochrome a occurs. These results are consistent with the branched pathway for the oxidase/O_2 reaction proposed by Hill and Greenwood (1984). Within the context of this scheme, the ferryl-oxo intermediate we have observed arises as the fourth and final electron enters the dioxygen reduction site.

To the memory of my Father,

my Mother, and Zoe

ACKNOWLEDGMENTS

I would like to thank Dr. Gerald T. Babcock for his friendship, encouragement, and guidance during the course of this work. I am also grateful to Drs. Katharine Hunt, Julius Kovacs, and Paul Parker for serving on my committee. Thanks also goes to Vada O'Donnell and Bill Draper for their efforts in the preparation of this manuscript. I also owe special thanks to Ron Haas and Deak Watters for technical services. Finally, I would like to thank all my fellow lab members for their general assistance.

TABLE OF CONTENTS

Page

LIST OF TABLES

LIST OF FIGURES

CHAPTER 1

GENERAL INTRODUCTION

The production of energy in the cells of aerobic organisms is based on the transfer of electrons through a series of redox proteins in the respiratory chain leading to the final reduction of oxygen to water (Figure 1.1). An essential element of this mechanism is cytochrome oxidase, the terminal enzyme in cellular respiration (Figure 1.2). This enzyme transfers electrons from the protein cytochrome c to oxygen and carries out the reduction of oxygen according to the overall reaction: 4 cytochrome c^{2+} + O_2 + 4 H^+ → 4 cytochrome c^{3+} + 2 H_2O. In eucaryotes, the components of the respiratory chain are located in the inner membrane of mitochondria, and the free energy released in redox reactions is used to generate a proton gradient across the membrane. The ATP synthase complex, present in the same membrane, catalyzes the synthesis of energy-rich ATP from ADP and phosphate with this proton gradient as the driving force. Thus, the mitochondrial respiratory chain and the

Figure 1.1 Sequence of electron carriers in the respiratory chain; approximate midpoint potentials of the components at pH 7 are indicated on the right side of the Figure.

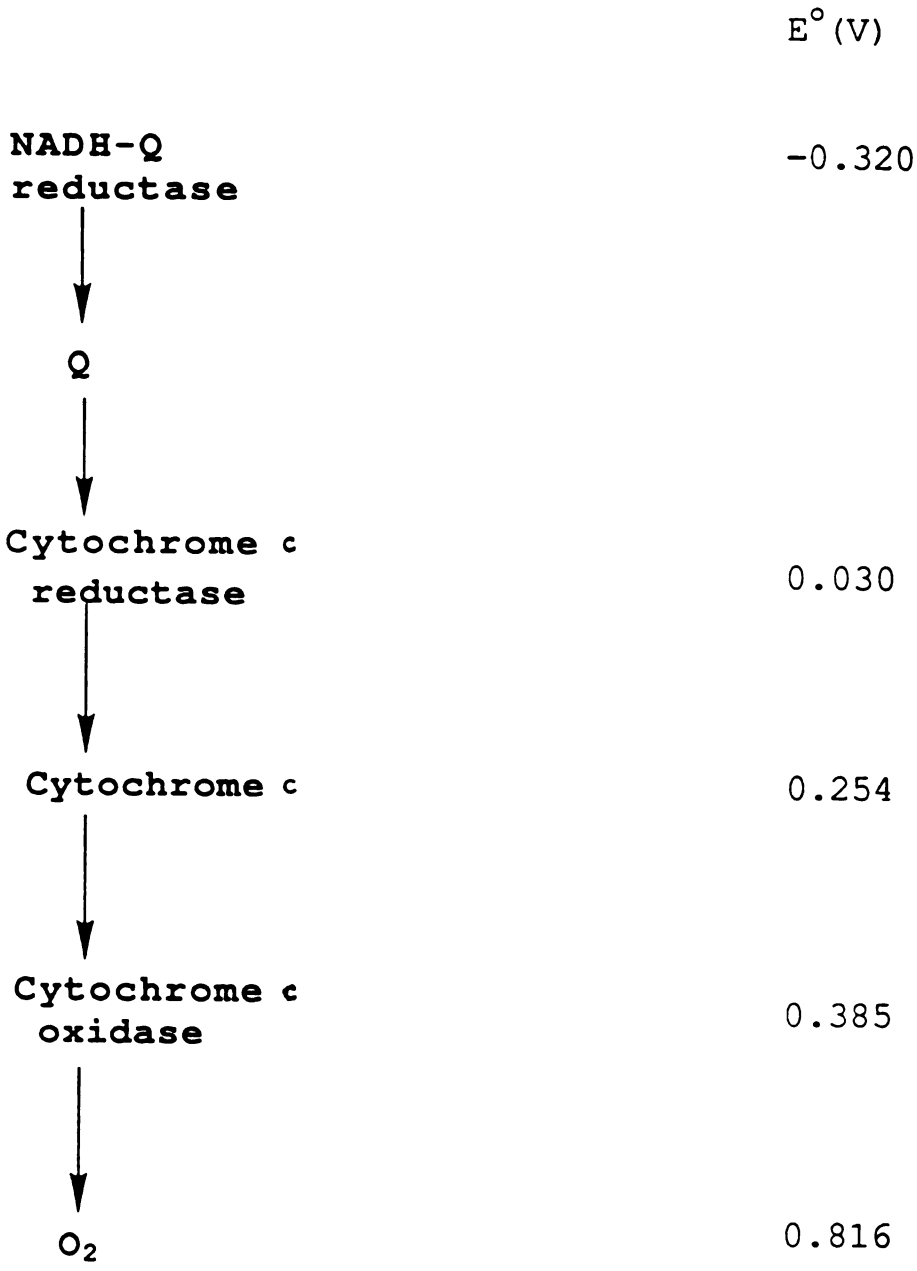

$$O_2 + 4H^+ + 4e^- \longrightarrow 2H_2O$$

Figure 1.2 The location of cytochrome oxidase in eucaryotic organisms. Adapted from Ref. 2a.

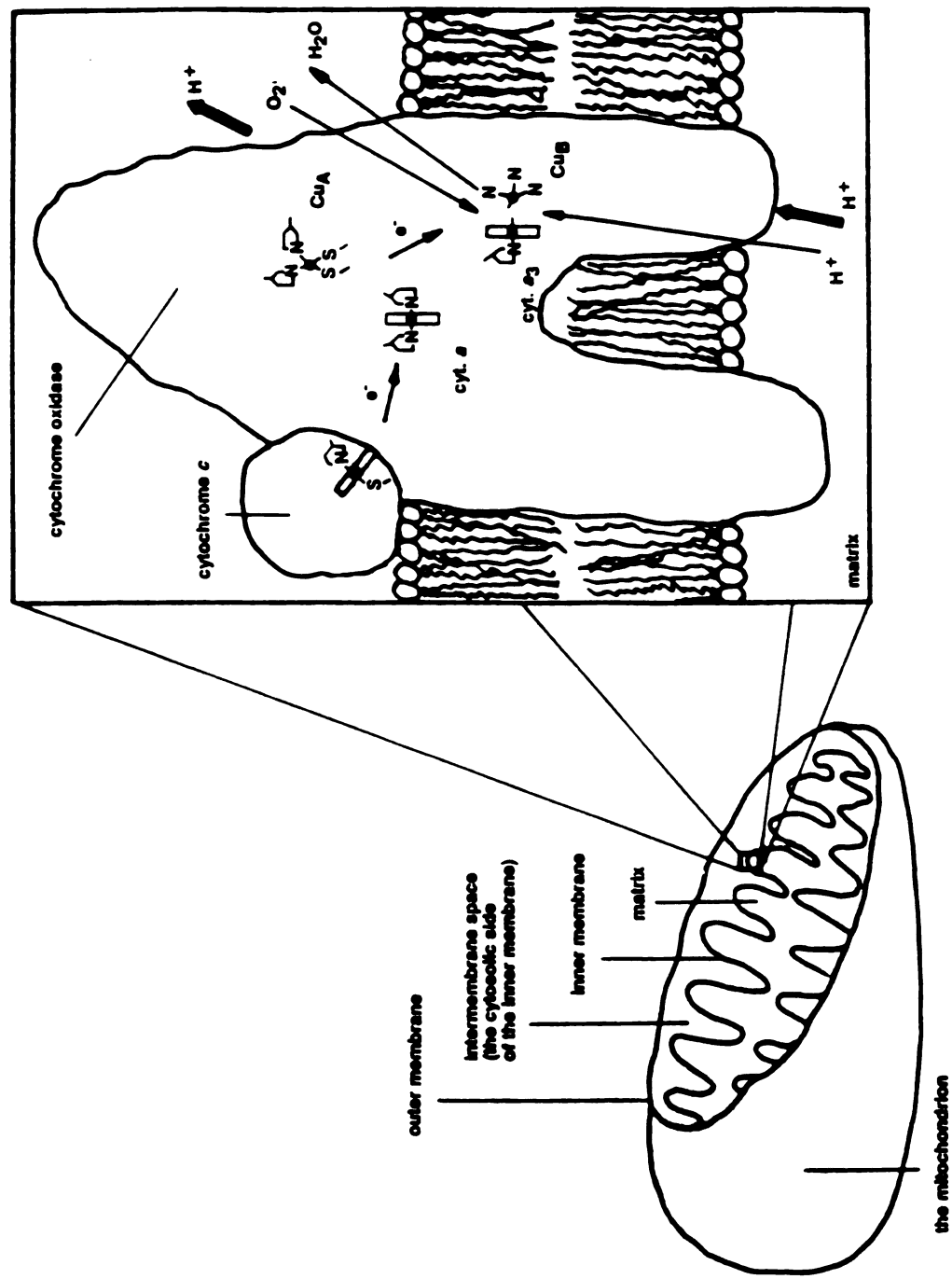
cytochrome oxidase
cytochrome c
matrix
H^+
O_2
H_2O
Cu_A
Cu_B
cyt. a
cyt. a_3
H^+
H^+
outer membrane
intermembrane space
(the cytosolic side
of the inner membrane)
inner membrane
matrix
the mitochondrion

ATP synthase complex supply the energy for the eucaryotic cell.

Cytochrome oxidase has at least eight subunits and a M.W of 140,000 Daltons.[1] Probably all of the redox metal centers are located in the two largest subunits (I and II). Subunit III has been implicated in the proton-translocating activity. Cytochrome oxidase contains four metal atoms per functional unit: two hemes, cytochrome a and a_3; and two associated copper atoms, Cu_A and Cu_B. The four redox active metals can be divided into two pairs. Cytochrome a and Cu_A function together in the sense that they accumulate electrons from cytochrome c and then act as a two-electron donor to the second pair metal ions, namely cytochrome a_3 and Cu_B. This second pair is present as a binuclear center that constitutes the catalytic site where oxygen binds and is reduced to H_2O.

I. The Individual Metals

Cytochrome a

In both oxidation states (II and III), the iron of cytochrome a remains low spin.[2b] It is characterized in its oxidized form by an EPR spectrum with g-values of 3.03, 2.213, and 1.5.[3] Comparison of these signals with those of model compounds suggested that, in the enzyme, this heme iron is coordinated to two neutral histidine residues.[4] Comparison of the resonance Raman spectra of cytochrome a and model compounds points to the same conclusions,[5] as does

the comparison of the MCD spectrum of bis-imidazole heme a and cytochrome a.[6]

Cu_A

The environment of this copper atom has been partially explained by the application of EPR[3,8] and ENDOR[9,10] spectroscopy together with the incorporation of ^{15}N into the enzyme isolated from yeast.[11a] These methods allowed the identification of one histidine and one cysteine as ligands, with the possibility of a second cysteine.

Cytochrome a_3 and Cu_B

The iron atom of cytochrome a_3 and its associated Cu_B form a coupled binuclear center. The most conspicuous spectroscopic feature of this interaction is the lack of EPR signals from the individual metals, even when they occur in their oxidized, paramagnetic states. This unusual situation arises from antiferromagnetic coupling between the high-spin ferric ion and the $Cu_B(II)$, forming a S = 2 EPR silent pair.[3,8,12] In the oxidized, resting enzyme, this coupling may be facilitated by a bridging ligand, possible identified by EXAFS as a chloride atom.[11b] Although EPR silent, cytochrome a_3 has been shown, from magnetic susceptibility[13] and MCD measurements,[14] to be high spin in the oxidized state and to remain so when reduced. Mossbauer spectroscopy[15a] confirms the high-spin nature of this ion; and, since no magnetic features are seen in the oxidized state at 4.2 K, supports the idea of spin coupling to a cupric ion.

Figure 1.3 Geometry and coordination properties for cytochrome a, cytochrome a_3, Cu_A, and Cu_B in cytochrome c oxidase. Adapted from Ref. 11c.

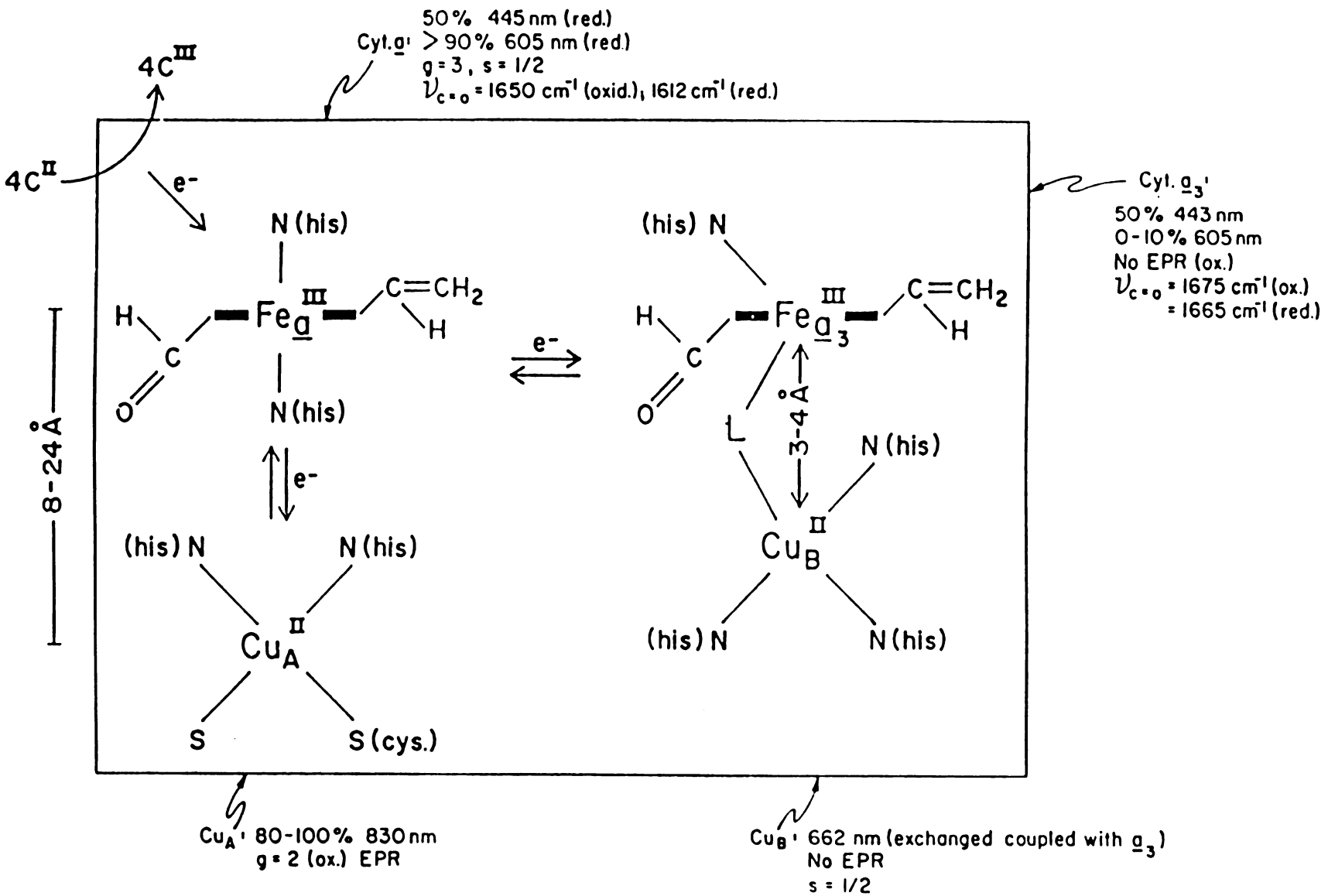
50% 445 nm (red.)
Cyt. a: >90% 605 nm (red.)
g = 3, s = 1/2
ν c=o = 1650 cm⁻¹ (oxid.), 1612 cm⁻¹ (red.)
4C III
4C II
e⁻
N (his)
H
C
O
Fe a III
C=CH2
H
N (his)
e⁻
(his) N
N (his)
Cu A II
S
S (cys.)
8-24 Å
(his) N
Fe a3 III
C=CH2
H
3-4 Å
L
N (his)
Cu B II
(his) N
N (his)
Cyt. a3
50% 443 nm
0-10% 605 nm
No EPR (ox.)
ν c=o = 1675 cm⁻¹ (ox.)
= 1665 cm⁻¹ (red.)
CuA: 80-100% 830 nm
g = 2 (ox.) EPR
CuB: 662 nm (exchanged coupled with a3)
No EPR
s = 1/2

Figure 1.4 A summary of current models for the coordination geometries of the iron and copper centers in reduced cytochrome oxidase. Adapted from Ref. 23.

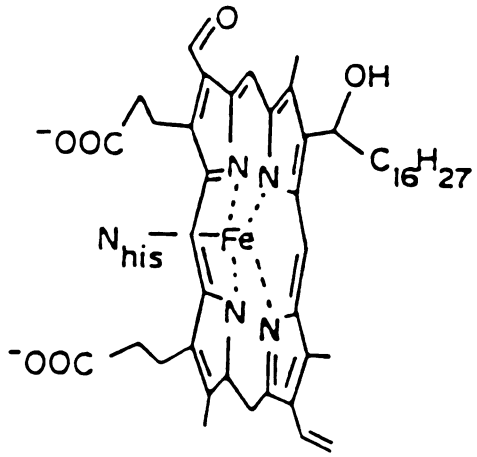

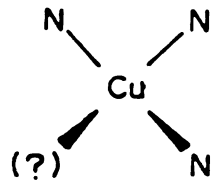

cyt $\underline{a}_3^{2+}$ | Cu_B^{1+}

$\underline{O_2}$ REDUCTION

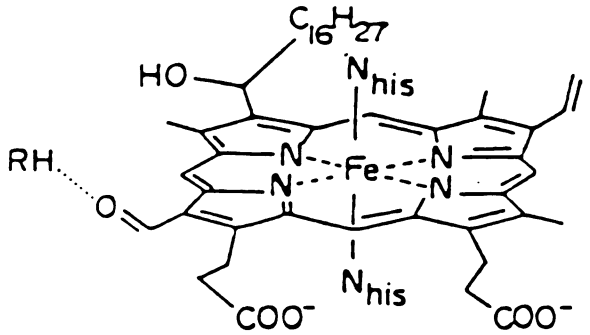

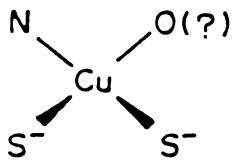

cyt $\underline{a}$ | Cu_A

CYTOCHROME $\underline{C}$ OXIDATION

II. Heme Absorption

The characteristics of the RR spectrum of a heme protein depend on the absorption band chosen in generating the RR effect. It is, therefore, necessary to outline the general characteristics of heme absorption spectra. The visible and near-ultraviolet absorption spectra of heme and metalloporphyrins are dominated by two $\pi \rightarrow \pi^*$ electronic transitions. Both transitions are polarized in the plane of the heme (x,y) and are of the same symmetry, E_u. The $\pi \rightarrow \pi^*$ transitions are subject to strong configuration interaction, with the result that the transition dipoles are additive for the higher energy transition and largely cancel for the lower-energy one. The higher-energy transition is assigned to the intense ($\varepsilon \sim 10^5$ M^{-1} cm^{-1}) absorption band, called the Soret or γ band, near 400 nm. The lower-energy transition is assigned to the α band, and has approximately tenfold less oscillator strength than the Soret transition. The lower-energy transition can "borrow" some of the intensity of the higher-energy transition through vibrational interactions. This produces a vibronic side band, called the β band, which occurs at an energy ~ 1300 cm^{-1} higher than the α band.

III. Optical Absorption of Cytochrome Oxidase

The spectrum of the fully-oxidized enzyme, as prepared, is characterized by broad absorption bands with peaks around 420 nm and 600 nm.[15b] The position of the Soret band is

Figure 1.5 Optical absorption spectra of cytochrome oxidase: oxidized—and fully reduced---- Adapted from Ref. 15c.

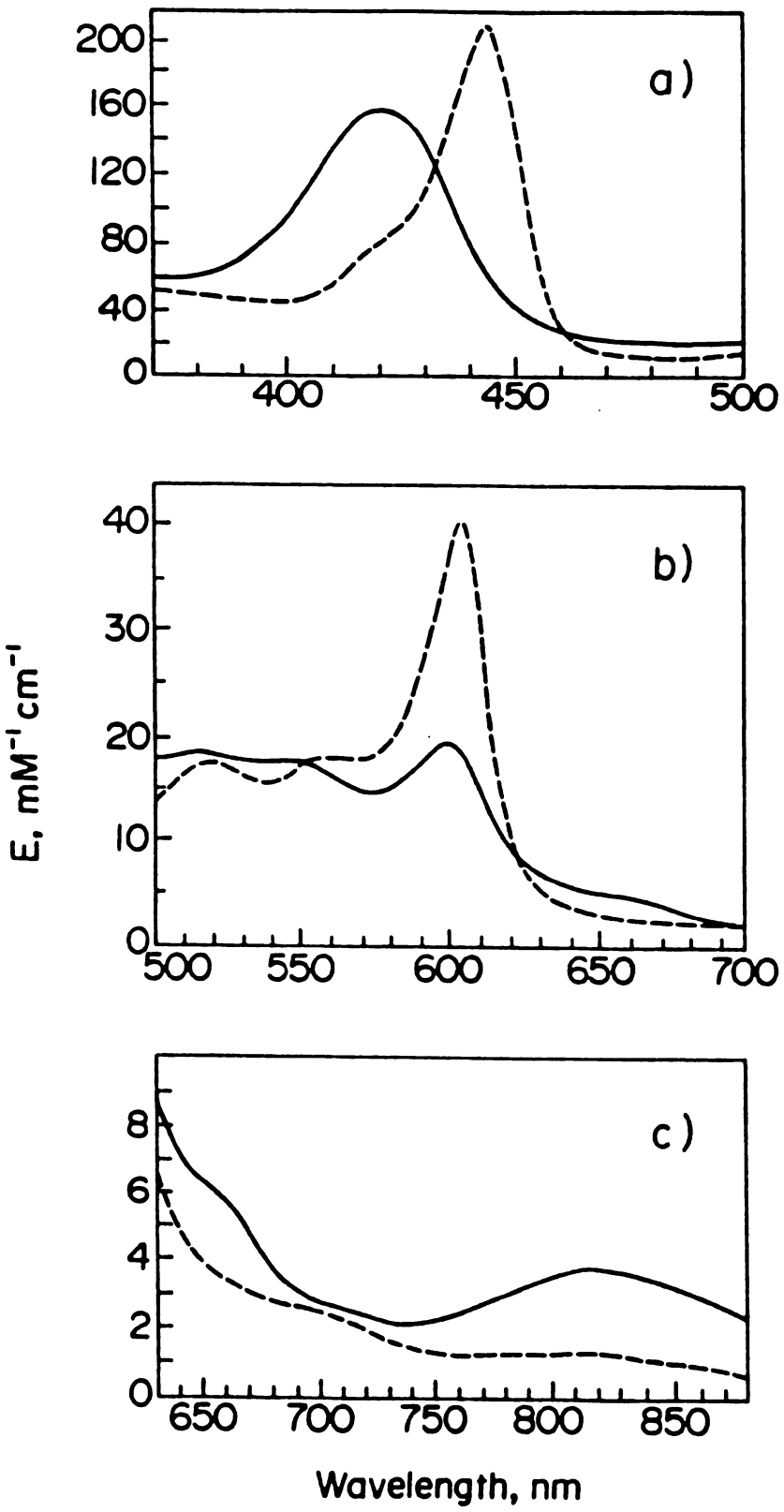
a)
b)
c)
E, mM⁻¹cm⁻¹
Wavelength, nm
200
160
120
80
40
0
400
450
500
40
30
20
10
0
500
550
600
650
700
8
6
4
2
0
650
700
750
800
850

variable, depending on the method of preparation. Other distinctive features of the oxidized enzyme are the broad band centered at 830 nm (Cu_A^{2+}) and a shoulder at 655 nm. On complete reduction of the enzyme, the Soret band shifts to 444 nm and the alpha band to 604 nm. The spectrum of cytochrome a is largely independent of the redox and ligation state of cytochrome a_3 and vice versa. Therefore, it has been possible to deconvolute the optical spectra and assign spectral properties to the individual centers. By using half-reduced states (i.e., enzyme species that have been prepared so that the hemes have different oxidation levels) and a variety of ligands for either ferrous or ferric cytochrome a_3, it has been shown that the cytochrome a makes the major contribution (80%) to the spectrum of the reduced enzyme at 605 nm, while the two cytochromes make approximately equal contributions at 444 nm. Carbon monoxide reacts with cytochrome oxidase only when both metals at the binuclear center are reduced, regardless of the oxidation state of cytochrome a and Cu_A. Carbon monoxide is bound only to ferrocytochrome a_3, whose absorption spectrum is characterized by a small decrease of the absorbance at 605 nm and new absorption bands at 592 and 430 nm.[16]

IV. Raman Theory

The Raman effect derives from the inelastic scattering of electromagnetic radiation by matter. The molecule is promoted to higher vibrational quantum levels of the ground electronic state during this process. Molecular spectroscopic information is conveyed by the vibrational frequency shift, by the intensity of the Raman scattering process, and by the polarization of the Raman scattered light relative to the incident radiation. The intensity of the scattered radiation I_{mn}, due to the transition from $|m\rangle$ to $|n\rangle$, is given by equation 1, where $(\alpha_{\rho\sigma})_{mn}$ is the transition polarization tensor with incident and scattered polarizations indicated by ρ and σ, respectively. The expression for $(\alpha_{\rho\sigma})_{mn}$ is given by equation 2. The polarizability expression has a contribution from all of the rovibronic molecular excited states, as indicated by the summation over the excited states $|e\nu\rangle$ in equation 2. The weighing of an individual $|e\nu\rangle$ excited state contribution is determined by the values of the transition moment matrix elements in the numerator and by the values of the energy denominators. The energy denominator contains information on $\Gamma_{e\nu}$, the homogeneous linewidth for the transition between the ground state m and the excited state $|e\nu\rangle$, and the detuning of excitation from resonance $(\nu_{ev}-\nu_0)$. For normal Raman scattering in which the excitation frequency is far

Figure 1.6 Diagram illustrating the resonance Raman effect

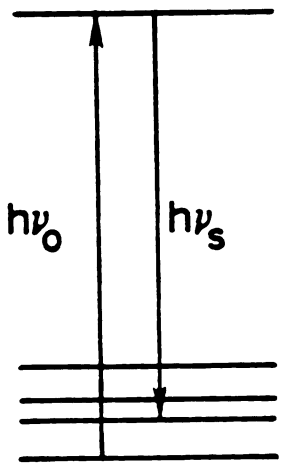

$$I_{mn} = \frac{128\,\pi^5}{9\,c^4}(\nu_0 \pm \nu_{mn})^4 I_0 \sum_{\rho\sigma} |(\alpha_{\rho\sigma})_{mn}|^2 \qquad 1$$

$$\alpha_{\rho\sigma} = \sum_{ev} \frac{\langle n|r_\rho|ev\rangle\langle ev|r_\sigma|m\rangle}{\nu_{ev}-\nu_0-i\Gamma_{ev}} + \frac{\langle n|r_\sigma|ev\rangle\langle ev|r_\rho|m\rangle}{\nu_{ev}+\nu_0-i\Gamma_{ev}} \qquad 2$$

$\alpha_{\rho\sigma} = A + B + C$:

$$A = \sum_{ev} \frac{\langle g|r_\rho|e\rangle\langle e|r_\sigma|g\rangle}{\nu_{ev}-\nu_0-i\Gamma_{ev}} (f|v)(v|i)$$

$$B = \sum_{ev} \left\{ \left[\frac{\partial\langle g|r_\rho|e\rangle}{\partial Q_a} \right]_0 \cdot \frac{\langle e|r_\sigma|g\rangle}{\nu_{ev}-\nu_0-i\Gamma_{ev}} \right\} (f|Q_a|v)(v|i)$$

$$+ \left(\frac{\langle g|r_\rho|e\rangle}{\nu_{ev}-\nu_0-i\Gamma_{ev}} \cdot \left[\frac{\partial\langle e|r_\sigma|g\rangle}{\partial Q_a} \right]_0 \right) (f|v)(v|Q_a|i)$$

$$C = \sum_{ev}\sum_{a}\sum_{b} \left(\left[\frac{\partial\langle g|r_\rho|e\rangle}{\partial Q_a} \right]_0 \left[\frac{\partial\langle e|r_\sigma|g\rangle}{\partial Q_b} \right]_0 \right) (f|Q_a|v)(v|Q_b|i).$$

from resonance with an electronic transition in the molecule, the denominator only weakly depends upon excitation frequency, and all molecular rovibronic transitions contribute essentially in proportion to their transition moments. As resonance with an electronic transition is approached, the first term in equation 2 begins to dominate the sum over states of the Raman polarizability expression. If we display the dependence of the transition moment matrix elements upon vibrational motion, we can show that equation 2 predicts three distinct scattering mechanisms, A, B, and C, as discussed in the following paragraphs.

The transition moment matrix elements have been factored into separate electronic and vibrational integrals. This is achieved within the Born-Oppenheimer approximation by writing the total wave-functions as products of electronic and vibrational parts. The change of the electronic wave-function, due to the origin shift, is incorporated by using the Herzberg-Teller expansion. The transition moment integrals between the ground and excited electronic states are denoted by angular brackets. Curved brackets denote the integrals between vibrational level, where $|i)$ labels the initial vibrational level of the normal mode a in the ground electronic state, and $|v)$ labels the vibrational level of mode a in the excited electronic state. $|f)$ labels the final vibrational level of mode a in the ground electronic state ($f = i+1$ for Stokes Raman scattering

from mode a). The Franck-Condon overlap factors $(f|v)(v|i)$ will differ from zero only if the excited state equilibrium geometry is displaced along a symmetric normal mode coordinate relative to the ground state. This assumes identical orthonormal vibrational wavefunctions in the ground and excited states.

A-term, Condon enhancement may also occur due to strong Franck-Condon overlaps when the excited state vibrational level are solutions to a different Hamiltonian than that of the ground state. For the more common case in large molecules of similar vibrational mode compositions in the ground and excited states, where the excited state geometry either expands or contracts relative to the ground state, the enhancement of totally symmetric vibrations scales roughly as $(\Delta)^2/_2$, where Δ is the magnitude of displacement of the excited state potential surface along the Raman active normal coordinate. For small displacements, only the fundamental shows significant enhancement. Larger displacements result in lengthy Franck-Condon progressions. Enhancement of symmetric vibrations by the A-term can also derive from vibrational force constant changes in the excited state as well as by alterations in the composition of the excited state normal coordinates (Duschinsky effect).

Enhancement via the B-term derives from the non-Condon dependence of the electronic transition moment upon the vibrational coordinate. One example of a non-Condon enhancement mechanism is Herzberg-Teller vibronic coupling

of different electronic transitions. Both symmetric and nonsymmetric fundamentals can be enhanced by a B-term mechanism for a strongly-allowed transition, the magnitude of B-term enhancement of symmetric vibrations is significantly below that for A-term enhancement. B-term enhancement will dominate only for the nonsymmetric vibrations.

If the transition is forbidden at the equilibrium geometry, enhancement of fundamentals cannot occur via either the A or B-terms; however, C-term enhancement of overtones and combinations can occur and will involve two quanta of vibrational mode a or the combination of one quantum of mode a and one quantum of mode b. The C-term only dominates enhancement for resonance excitation within forbidden electronic transitions.

Resonance Raman studies of porphyrins provide an important correlation between the position of given vibrations and the oxidation and spin states of the central metal. The resonance Raman results for cytochrome oxidase discussed in this chapter are primarily those obtained with Soret excitation. Under this condition, the Franck-Condon mechanism dominates RR scattering, and all observed RR modes are polarized (ρ ~ 0.33). The vibrations in the 1000-1700 cm^{-1} region represent primarily C-C and C-N stretching motions of the hemes. The following discussion concentrates on two primary RR indicator bands of cytochrome oxidase. The first is the ν_4 symmetric vibration in the 1355-1375

cm^{-1} region, the frequency of which is sensitive to electron density in porphyrin π^* orbitals. In practice, ν_4 is sensitive to two effects: the oxidation state of the metal and the presence of axial ligands that have π-acid character and, thus, may withdraw porphyrin π^*-electron density via the metal. The second RR indicator band is the ν_2 vibration which behaves as a reliable core-size indicator. Therefore, the lowering of the heme frequencies reflects expansion of the heme. A detailed analysis of several high- and low-frequency vibrations in cytochrome oxidase will be discussed in Chapters 3, 4, and 5.

V. Oxygen Intermediates

In 1958, Okunuki[17] reported that when O_2 is added to the reduced-cytochrome oxidase, the Soret shifts to 428 nm. This newly-observed species was termed "oxygenated" and was believed to be an oxygen compound of cytochrome oxidase similar to oxyhemoglobin. It is now known that this simple view is incorrect and that reduced cytochrome oxidase reacts with O_2 in approximately 1 ms at room temperature to regenerate the fully-oxidized enzyme.[18] Because the reaction is extremely fast, manual stopped flow is not reliable; instead the O_2 site can be blocked with CO. The CO dissociates slowly in the absence of light ($k=2.5\times10^{-2}s^{-1}$) so that an anaerobic sample treated with CO can be mixed with O_2 under conditions for which no significant reaction with oxygen occurs (30 sec) until a

short light pulse is used to photodissociate the CO.

Gibson and Greenwood[18] studied the reaction of reduced cytochrome oxidase with O_2 by combining rapid mixing and flash photolysis, which provided resolution on the microsecond timescale. This "flow-flash" technique involves mixing the CO-bound reduced enzyme with O_2 and then subjecting the mixture to an intense flash of light. The flash photolyzes the heme-CO bond to produce the unbound reduced enzyme free to react with O_2. Gibson and Greenwood proposed a model (Figure 7) suggesting that the initial bimolecular step is a combination of the enzyme with O_2 in which O_2 is not bound, as an inner-sphere ligand, to cytochrome a_3, but instead is trapped in the protein pocket. The second step is an intramolecular step occurring at a first-order rate of $6x10^4 s^{-1}$ resulting in the transfer of O_2 to its metal binding site at cytochrome a_3, which corresponds, in Chance's notation, to compound A formation. The kinetic difference spectra generated in the O_2 reaction may be reconciled with those from the static and reducive kinetic experiments by having about 40% of the cytochrome a oxidized with $t_{1/2} \sim 35\ \mu s$.[18] Such a suggestion requires a branch in the pathway of the reaction of the fully-reduced enzyme with O_2.

The scheme of Figure 7 suggests that the first event

Figure 1.7 Reaction mechanism of fully-reduced cytochrome oxidase obtained by flash photolysis at room temperature. Adapted from Ref. 18

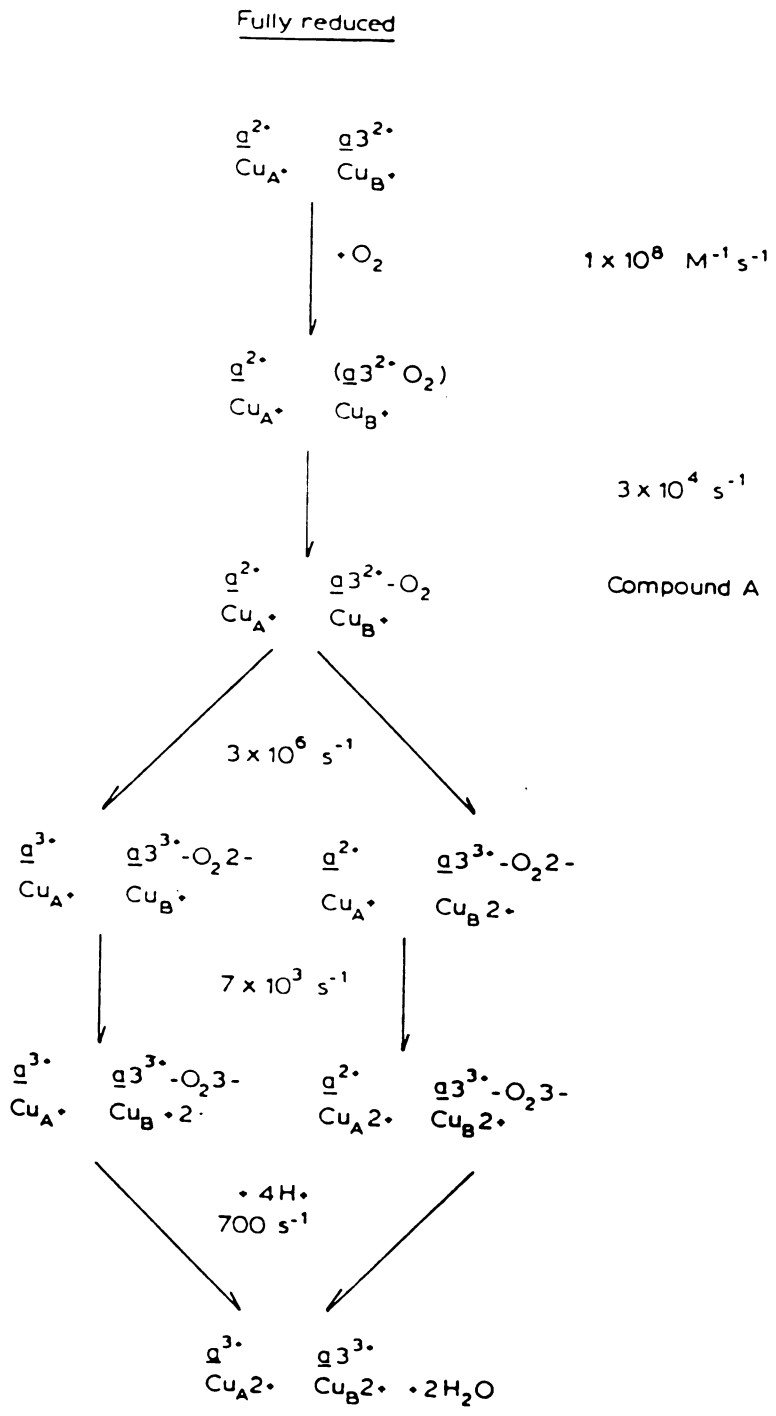
Fully reduced
a2+ a32+
CuA+ CuB+
+O2
1 x 10^8 M^-1 s^-1
a2+ (a32+ O2)
CuA+ CuB+
3 x 10^4 s^-1
a2+ a32+-O2
CuA+ CuB+
Compound A
3 x 10^6 s^-1
a3+ a33+-O2 2-
CuA+ CuB+
a2+ a33+-O2 2-
CuA+ CuB 2+
7 x 10^3 s^-1
a3+ a33+-O2 3-
CuA+ CuB +2
a2+ a33+-O2 3-
CuA 2+ CuB 2+
+4H+
700 s^-1
a3+ a33+
CuA 2+ CuB 2+ +2H2O

after O_2 binding is the transfer of two electrons to form a peroxo intermediate. It is at this stage that the branch is introduced. The two electrons transferred in this step may originate from either cytochrome a_3 and Cu_B or from cytochrome a_3 and cytochrome a. This heterogeneity may simply be a manifestation of an intrinsic difference in the rates of electron transfer from different metal centers in the enzyme to bound O_2. The second electron-transfer step involves the oxidation of Cu_A, as evidenced by the change at 830 nm. There is evidence, from spectroscopic potentiometric-titration experiments, that the 830 nm band is nearly entirely due to Cu_A.[19,20] The observed ratio of the fast/slow phases at 830 nm is 60:40, as predicted by the proportion in each branch necessary to account for the cytochrome a and a_3 absorption contributions in the Soret and visible regions. Therefore, the branching model is able to account for the complex kinetics at 830 nm and retain Cu_A as the sole chromophore contributing at this wavelength. This result also suggests that interconversion between the two branches must be slow, relative to the rates of the individual steps in the branches. The second and third electron-transfer steps in each branch are shown to occur at identical rates. This implies that the rate limit to electron transfer within the complex is imposed by a shared event such as the binding of protons.

Chance et al.[21a] developed techniques to study the reaction on a second-to-minute time scale at low

temperature. With this approach, Chance et al.,[21a] Clore et al.,[21b] and Chan et al.[21c] studied intermediates involved in dioxygen reduction and characterized them by using optical and EPR spectroscopies. Chan et al.[21c] confirmed the earlier findings of Clore et al.[21b] about the initial phases of the reaction involving the binding of O_2 to form compound A and subsequent heterogeneous reaction of both Cu_A and Cyt a. They also show that the kinetics of the appearance of the EPR signal assigned to Cu_B are correlated to electron transfer from either Cu_A or Cyt a. These workers suggest that the decay of the Cu_B signal may be correlated to the breaking of the dioxygen bond.

Although Gibson and Greenwood studied the absorption changes during the O_2 reaction of reduced cytochrome oxidase by the rapid-reaction technique of flow-flash spectrophotometry in the Soret, visible and near i.r. spectral region, their data do not provide direct spectroscopic evidence to support the proposed structures for the various intermediates shown in Figure 7. Time-resolved resonance Raman spectroscopy provides a variety of advantages over time-resolved absorption spectroscopy. It offers not only the possibility of detecting the out-of-plane ligand vibrational modes and, thus, the structure of the bound O_2 species through isotopic labeling of the O_2, but information concerning heme geometric and electronic properties as well. Changes in these molecular parameters at the protein-active site can then be used to test whether

Figure 1.8 Postulated intermediates in the reduction of O_2 by cytochrome oxidase. Only the a_3/Cu_B site is shown. L represents a bridging ligand in the oxidized form of the enzyme. Adapted from Ref. 23.

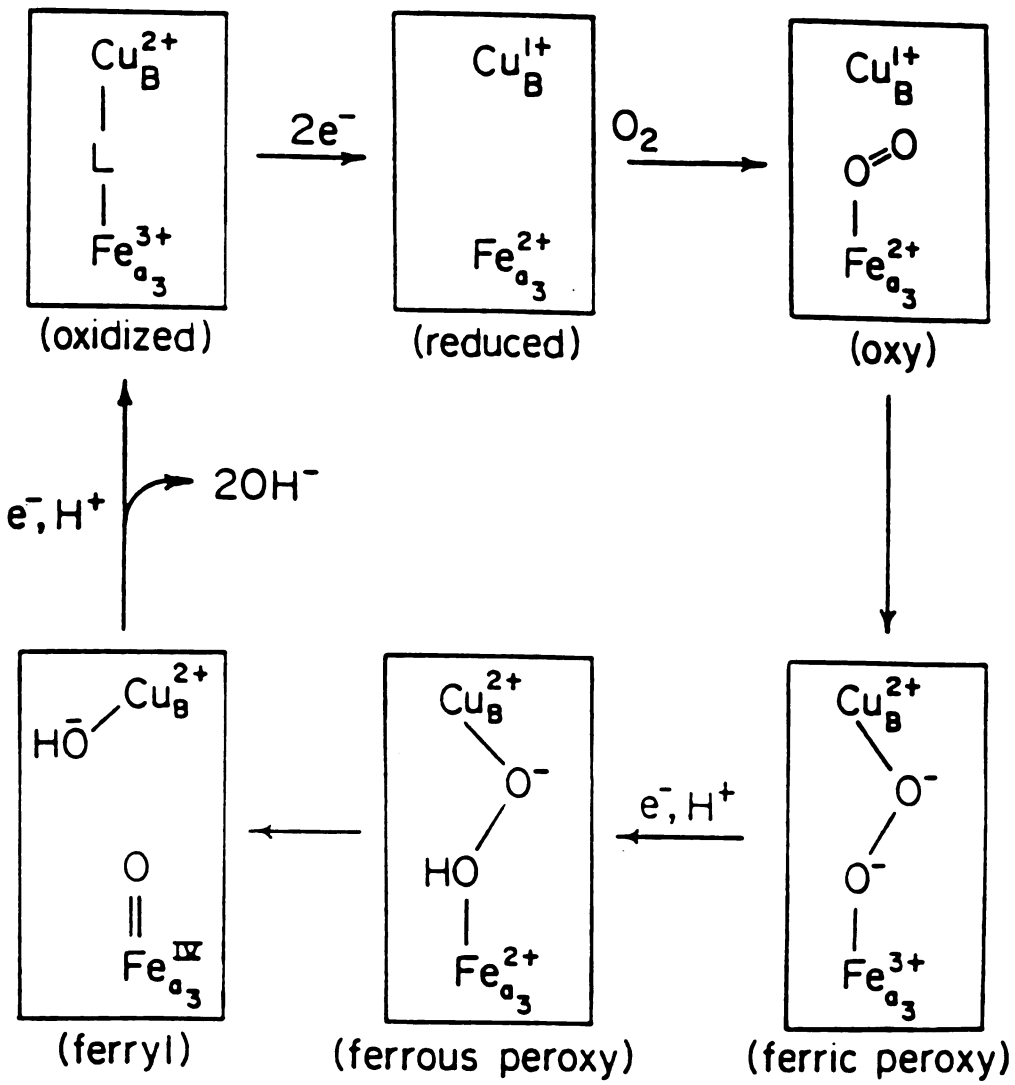
Cu$_B^{2+}$
L
Fe$_{a_3}^{3+}$
(oxidized)
2e$^-$
Cu$_B^{1+}$
Fe$_{a_3}^{2+}$
(reduced)
O$_2$
Cu$_B^{1+}$
O=O
Fe$_{a_3}^{2+}$
(oxy)
e$^-$, H$^+$
2OH$^-$
HO
Cu$_B^{2+}$
O
Fe$^{IV}_{a_3}$
(ferryl)
Cu$_B^{2+}$
O$^-$
HO
Fe$_{a_3}^{2+}$
(ferrous peroxy)
e$^-$, H$^+$
Cu$_B^{2+}$
O$^-$
O$^-$
Fe$_{a_3}^{3+}$
(ferric peroxy)

the postulated structures in Figures 7 and 8 do, in fact, occur.

Babcock et. al.[22-23] used two-color, time-resolved resonance Raman spectroscopy on flowing samples prepared by rapid mixing to study the reaction of fully- and partially-reduced cytochrome c oxidase with dioxygen. Although instrumental limitations restricted data acquisition to the high-frequency (>1000 cm^{-1}) range, they concluded that the dioxygen reduction proceeds via a photolabile oxycytochrome a_3 complex which has characteristics similar to oxyhemoglobin and oxymyoglobin. Moreover, they postulated that these intermediate species were replaced by nonphotolabile dioxygen adducts in which cytochrome a_3 was oxidized with $t_{1/2}$~60μs and $t_{1/2}$~200μs in the fully-reduced and mixed-valence complexes.

The aim of this work is to characterize the vibrational and structural properties of the intermediates formed in the reactions of dioxygen with fully-reduced and mixed-valence cytochrome oxidase by using time-resolved resonance Raman spectroscopy in conjunction with rapid-mixing/flow techniques applied to the enzyme.

REFERENCES

1. M. Wikstrom, K. Krab, and M. Saraste, "Cytochrome Oxidase, A Synthesis", Acad. Press, New York, 1981.
2. a) P. E. Thornstrom (1988), Ph.D. Thesis, University of Goteborg and Chalmers University of Technology. b) K. E. Falk, T. Vanngard, and J. Angstrom, FEBS Lett. 75, 23 (1977).
3. C. R. Hartzell and H. Beinert, Biochim. Biophys. Acta, 368, 318 (1974).
4. W. E. Blumberg and J. Peisach in "Cytochrome Oxidase", T. E. King, Y. Oni, B. Chance, and K. Okunuki, Eds., Elsevier, Amsterdam, 1979, p. 153.
5. G. T. Babcock, P. M. Callahan, M. R. Ondrias, and I. Salmeen, Biochemistry 20, 959 (1981).
6. D. G. Eglinton, B. D. Hill, C. Greenwood, and A. J. Thomson, J. Inorg. Biochem. 21, 1 (1984).
7. M. T. Wilson, C. Greenwood, M. Brunori, and E. Antonini, Biochem. J. 147, 145 (1975).
8. R. Aasa, S. P. J. Albracht, K. E. Falk, B. Lanne, and T. Vanngard, Biochim. Biophys. Acta 442, 260 (1976).
9. B. M. Hoffman, J. K. Roberts, M. Swanson, S. H. Speck,

and E. Margoliash, Proc. Natl. Acad. Sci. USA 77, 1452 (1980).

10. H. L. VanCamp, J. H. Wei, C. P. Scholes, and T. E. King, Biochim. Biophys. Acta 537, 238 (1978).

11. a) T. H. Stevens, C. T. Martin, H. Wang, G. H. Brudvig, C. P. Scholes, and S. I. Chan, J. Biol. Chem. 257, 12106 (1982); b) R. Scott, M. Li, and S.-I. Chan (1988), Annals of the New York Academy of Science 550, 53-58; c) J. Centeno (1988), Ph.D. Thesis, Michigan State University.

12. G. Palmer, G. Babcock, L. Vickery, Proc. Natl. Acad. Sci. U. S. A. 73, 2206-2210 (1976).

13. M. Tweedle, L. J. Wilson, L. Garcia-Iniquez, G. T. Babcock, and G. Palmer, J. Biol. Chem. 253, 8065 (1978).

14. a) G. T. Babcock, L. E. Vickery, G. Palmer, J. Biol. Chem. 251, 7907 (1976); b) A. J. Thomson, T. Brittain, C. Greenwood, and J. P. Springill, Biochem., J. 165, 327 (1977).

15. a) T. A. Kent, L. J. Young, G. Palmer, J. A. Fee, and E. Munck, J. Biol. Chem. 258, 8543 (1983). b) Vanneste, W. H., Biochemistry 5, 838-847 (1966); c) F. G. Halaka (1981), Ph.D. Thesis, Michigan State University.

16. J. Tang and A. C. Albrecht in "Raman Spectroscopy Theory and Practice" (ed. H. A. Szymanski), Vol. 2, pp. 33-68; D. L. Rousseau and P. C. Williams in "Topics in

Current Physics", Vol. 2, "Raman Spectroscopy of Gases and Liquids" (Ed. A. Weber); R. J. H. Clark and B. Stewart, Struct. and Bonding 36, 1 (1979).

17. K. Okunuki, B. Hagihara, I. Sekuzu, T. Horio, Proc. Int. Symp. Enz. Chem. 264 (1958).

18. Q. H. Gibson, C. Greenwood, Biochem. I. 86, 541 (1963); Q. H. Gibson, C. Greenwood, Biol. Chem. 240, 2694 (1965); C. Greenwood, B. Hill, Biochem. J. 218, 913 (1984); for review see: B. Hill, C. Greenwood, P. Nichols, Biochim. Biophys. Acta 91, 853 (1986) and A. Nafui and B. Chance, Ann. Rev. Biochem. 55, 137 (1986).

19. G. T. Babcock, L. E. Vickery, and G. Palmer (1978), J. Biol. Chem. 253, 2400-2411.

20. H. Beinert, R. W. Shaw, R. E. Hansen, and C. R. Hartzell (1980), Biochim. Biophys. Acta 591, 458-470.

21. a) B. Chance, C. Saronio, and J. S. Leigh, J. Biol. Chem. 250, 9226-9237 (1975); b) G. M. Clore, L. E. Andreasson, B. Karlsson, R. Aasa, and B. G. Malmstrom, Biochem. J. 185, 139-154 (1980); c) S. I. Chan, S. N. Witt, and D. F. Blair, Chemica Scripta 28A, 51-56 (1988).

22. G. T. Babcock, J. M. Jean, L. N. Johnston, G. Palmer, and W. H. Woodruff, J. Am. Chem. Soc. 106, 8305-8306 (1984).

23. G. T. Babcock, J. M. Jean, L. N. Johnston, W. H. Woodruff, and G. Palmer, J. Inorg. Biochem. 23, 243-251 (1985).

CHAPTER 2

A SIMPLE MIXER/JET CELL FOR RAMAN SPECTROSCOPIC STUDIES*

SUMMARY

A unique rapid mixing/jet apparatus that allows light scattering from a sample jet in air was constructed and applied successfully to observe low and high frequency resonance Raman spectra of the oxygen metabolizing heme protein, cytochrome oxidase. The cell is designed to minimize sample consumption and is well suited to pulsed laser excitation and to multichannel detection. To illustrate some of the features of the cell design resonance Raman spectra obtained with the mixer/quartz capillary and those obtained with the mixer/jet cell are compared.

---

*Varotsis, C.; Oertling W. A.; and Babcock, G. T., 1990, App. Spectroscopy, in press.

INTRODUCTION

In biological applications of resonance Raman spectroscopy it is frequently desirable to reduce the instantaneous and long term power density of the focused laser beam in order to preserve the sample. Both flowing sample methods and laser beam defocusing techniques have been used successfully by various groups to minimize damage to photolabile samples.[1-4] The use of flowing sample cells under conditions in which sample recycling is practical has the additional advantage that long acquisition times can be achieved with fairly minimal scattering consumption. Nonetheless, the flowing cells described to date are most useful when both fairly large volumes of sample are available and recycling is feasible. A further consideration with Raman flow cells involves the sample containment technique in the sample volume. Quartz capillaries are often used, but with these, quartz scattering is severe in the low frequency region, where it overlaps vibrational modes of the sample and makes their detection difficult. Several groups have avoided this problem by arranging their flowing cells so that the sample forms a free jet in air in the scattering volume (e.g. ref. 1, 2). A notable example of this is the microdroplet mixing technique developed by Kincaid and coworkers[2] in which both rapid mixing and Raman scattering take place in air and is compatible with continuous wave laser excitation.

The necessity of developing the Raman cell described in this report arose when we tried to use pulsed laser excitation to observe resonance Raman scattering of photolabile intermediates formed in the irreversible, reduction of O_2 by cytochrome oxidase. Because the reaction is irreversible each protein aliquot can be sampled only once, which necessarily precludes recycling. Thus, a major concern in the construction of the cell was to maximize the information we could obtain per sample aliquot. An additional objective was to be able to collect scattered light in the low frequency region efficiently as the most useful vibrations of the bound dioxygen substrate occur in this region. In the design that resulted we are able to achieve the following: (1) efficient mixing at low flow rates by using a modified eight jet Gibson type mixer[3] and (2) a continuous flow of sample in air in the scattering volume at flow rates as low as 0.2 ml/min. At this flow rate and with a laser pulse repetition rate of 10 Hz, 1.2 scattering volumes pass between pulses, which insures that each laser pulse is incident on a fresh sample aliquot. With these flow and laser pulse frequency parameters, the total sample volume required per laser shot is 0.33 $\mu\ell$. Moreover, we are able to obtain Raman spectra with good resolution at laser pulse energies as low as 0.3 mJ. With this approach we have avoided photolysis of the transient intermediates and have detected Raman spectra of the first of these species.[4] Finally, because the sample

is not contained by a quartz capillary in the scattering region, we are able to use multichannel detection to observe low frequency, as well as high frequency, spectra.

CELL DESCRIPTION AND PERFORMANCE

The design of the mixer/jet cell is shown in Figure 2.1. The exit port of the mixer is constructed so as to allow the flowing sample solution to form a continuous flow in air in the scattering volume, which eliminates quartz scattering. The continuous flow of sample is formed by two 0.66 mm i.d. glass micropipets. The mixer with the upper micropipet and the lower micropipet are each mounted on X-Y-Z translators, which allows us to optimize the stability of the jet. Generally, we find that a gap of ~2 mm is appropriate. The iris diaphragm is also mounted on an X-Y-Z positioner and serves as the laser beam waist controller. The translation stage on which the cell is mounted allows X, Y and Z movements relative to the entrance slit of the spectrometer.

To illustrate the performance of the cell, and particularly the advantages of the jet in overcoming the quartz scattering problem we show in Figure 2.2 and Figure 2.3 the resonance Raman spectra of the heme protein, cytochrome oxidase, in its oxidized state. This enzyme exhibits vibrational modes in the 200-1700 cm^{-1} region that arise from the heme macrocycle and, under certain

Figure 2.1 Apparatus for room-temperature resonance Raman spectra of rapidly-mixed/flowing samples

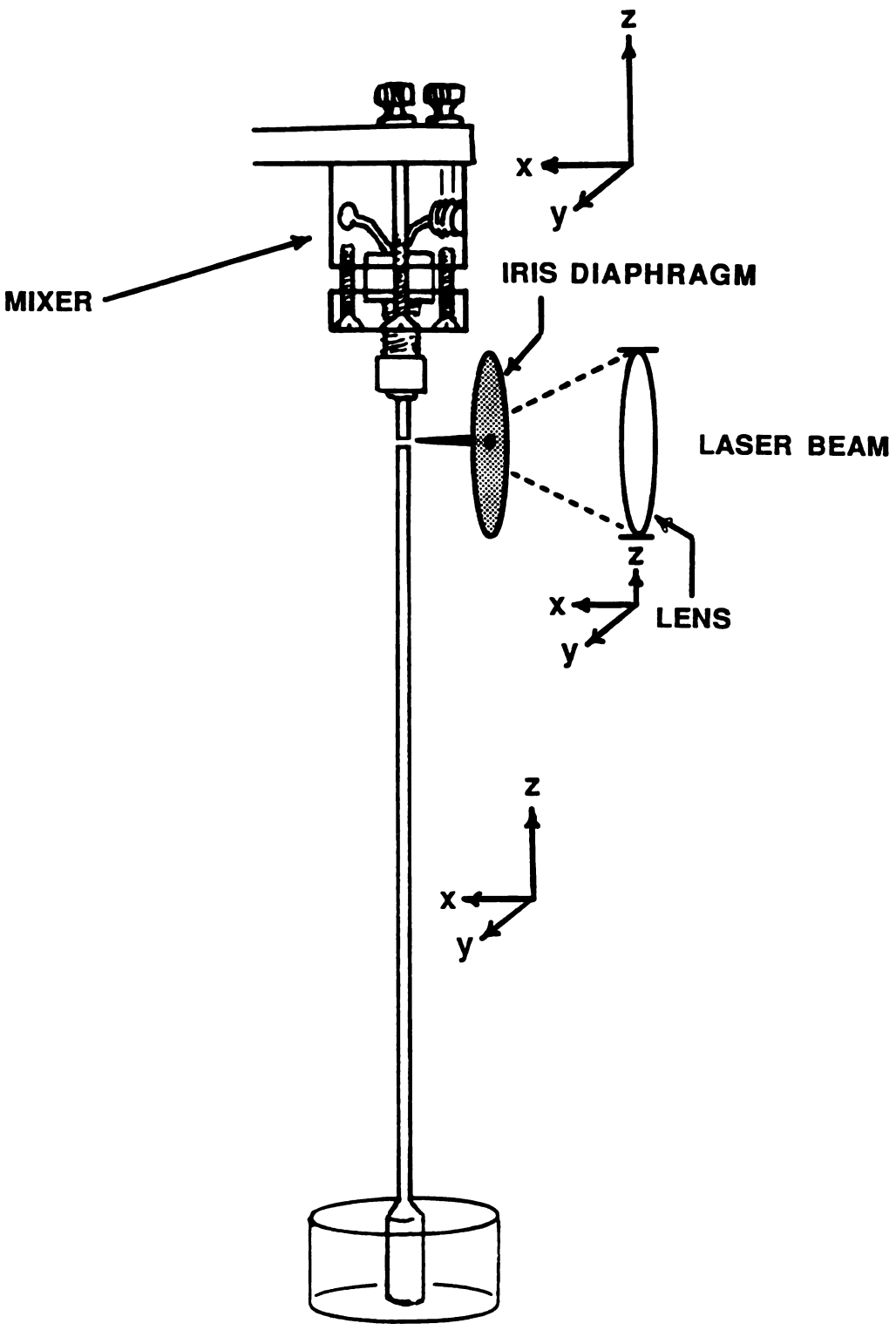
z
x
y
MIXER
IRIS DIAPHRAGM
LASER BEAM
z
x
y
LENS
z
x
y

conditions, from iron-axial ligand motions. Resonance Raman excitation at 416 nm is produced by Stokes Raman shifting the third harmonic of a Nd: YAG laser in H_2. Typical incident average powers were on the order of a few milliwatts (10 Hz) at this wavelength. The scattered radiation was collected with a SPEX 1877 Triplemate and detected by an EG & G PAR 1420 diode array detector. The resonance Raman spectra of oxidized cytochrome oxidase shown in Figure 2.2 and Figure 2.3 were recorded under identical conditions (laser power, sample concentration, and flow rate) with the exception that for spectra A a quartz capillary was used while spectra B were recorded with the mixer/jet cell described above. In the high frequency region (Figure 2.2) cytochrome oxidase displays Raman vibrations that are strongly enhanced with the Soret electronic transition. These arise from in plane ring modes that are coupled to π - π^* electronic transitions. The performance differences for the two scattering arrangements are apparent in the spectra. The vibrational modes at 1372, 1478, 1573, 1590, 1645, 1651, and 1675 cm^{-1}, which are clear in (B), lose resolution and apparent intensity in the spectrum obtained with the quartz capillary (A).

The most direct way of probing the bonding to the iron atom in a heme protein is to monitor the iron-ligand vibrations, which occur below 700 cm^{-1}. Unfortunately, these out-of-plane vibrations are not strongly enhanced by

Figure 2.2 High-frequency resonance Raman spectra of oxidized cytochrome oxidase. Spectrum A was recorded with a quartz capillary. Spectrum B was obtained with the mixer/jet cell. The energy of the 416 nm excitation wavelength was 0.8 mJ. The accumulation time was 2.5 min for both spectra and the flow rate was 0.2 ml/min. The sample concentration was 80 μM.

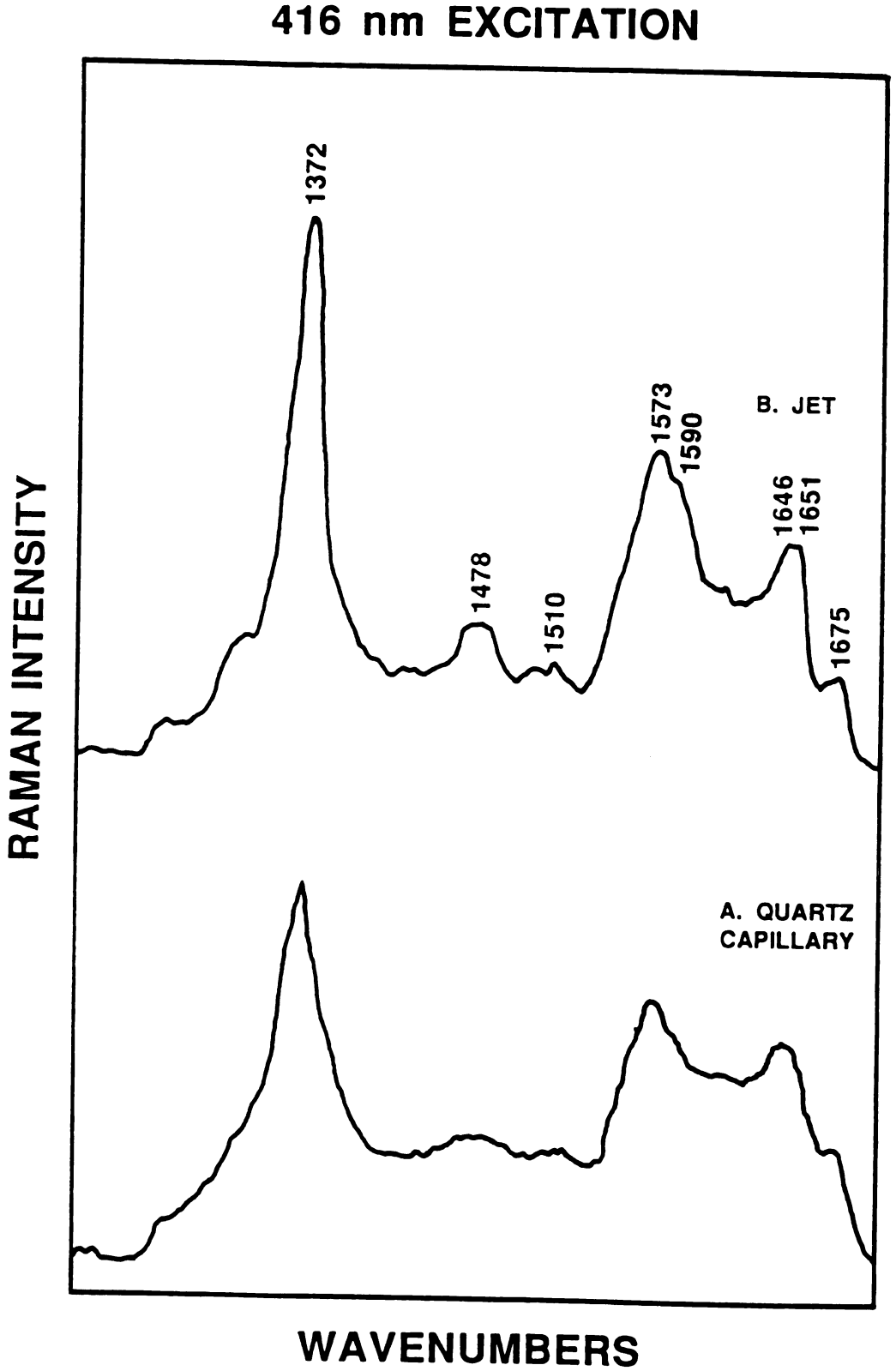
416 nm EXCITATION
RAMAN INTENSITY
1372
1478
1510
1573
1590
1646
1651
1675
B. JET
A. QUARTZ CAPILLARY
WAVENUMBERS

the dominant in-plane π - π^* electronic transitions. Nonetheless, the low-frequency resonance Raman spectrum holds considerable promise for quantifying bond strain and changes in length for the axial ligand linkages and is a major focus in a number of resonance Raman investigations of heme proteins. The 200 - 700 cm^{-1} region of the resonance Raman spectrum of resting cytochrome oxidase is shown in Figure 2.3. Table 2.1 compares and summarizes the frequencies observed with the mixer/jet and with the mixer/quartz capillary. There are significant differences in intensity between the resonance Raman spectra observed with the two devices, with a clear improvement in the signal-to-noise ratio of all the Raman modes in the spectrum taken with the mixer/jet arrangement.

Of particular importance is the fact that the lower frequency region (<300 cm^{-1}) shown in Figure 2.3A sits atop a broad baseline that is due to quartz scattering, which makes the detection of vibrational modes with frequencies between 150 and 300 cm^{-1} especially difficult. This is unfortunate because the ligand binding and dissociation pathways of heme proteins involve changes in the heme core size. This, in turn, depends on iron motion out of plane and hence on motion in the Fe-axial histidine bond. Thus, time-resolved resonance Raman studies of the Fe-his bond provide a direct means by which to monitor heme relaxation dynamics. However, the Fe-his stretching vibration occurs in the 200-240 cm^{-1} region for most heme proteins,

Figure 2.3 Low-frequency resonance Raman spectra of oxidized cytochrome oxidase. Spectrum A was recorded with a quartz capillary. Spectrum B was obtained with the mixer/jet cell. The energy of the 416 nm excitation wavelength was 0.8 mJ. The accumulation time was 2.5 min for both spectra and the flow rate was 0.2 ml/min. The sample concentration was 80 μM.

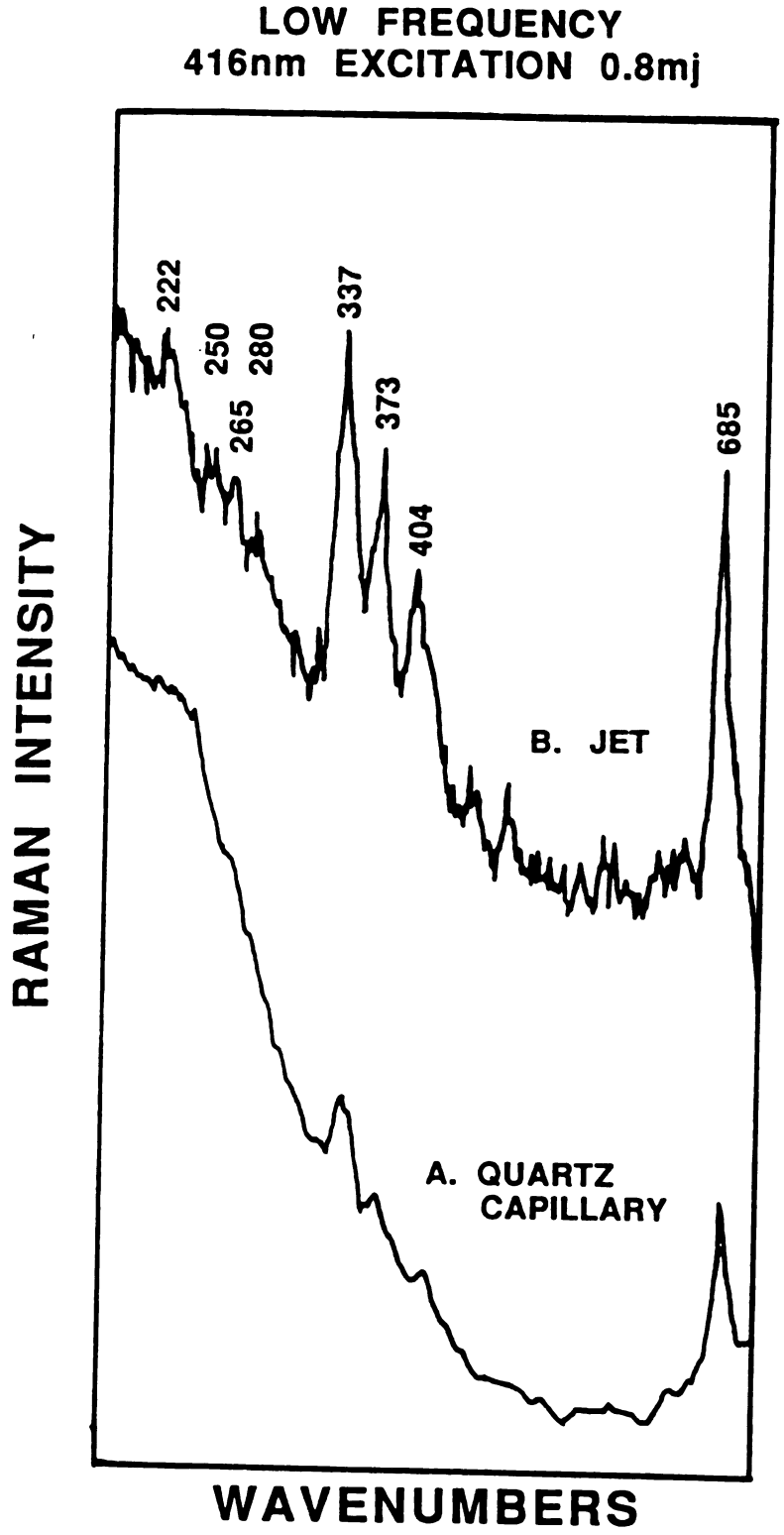
LOW FREQUENCY
416nm EXCITATION 0.8mj
222
250
280
265
337
373
404
685
B. JET
A. QUARTZ
CAPILLARY
RAMAN INTENSITY
WAVENUMBERS

Table 2.1

Low Frequency Raman modes (cm^{-1}) in Cytochrome Oxidase

Mixer/Jet	Quartz Capillary
222/w	–
250/w	–
265/w	–
280/w	–
337/s	337/w
373/s	373/w
404/s	404/w
685/vs	685/s

Abbreviations:

w - weak

s - strong

vs - very strong

including cytochrome oxidase.[5,6] Thus the quartz capillary design is unlikely to be useful in monitoring this important motion. The mixer/jet arrangement clearly circumvents the quartz scattering problem as shown in Figure 2.3B and thus opens to us the possibility of studying ν(Fe-his) as a function of time.

The data shown in Figure 2.2 and Figure 2.3 illustrate the unique opportunity of using multichannel techniques to observe Raman spectra of biological molecules in both the high and low frequency region without requiring high laser power levels or long sampling times. Moreover, small quantities of material are readily sampled.

REFERENCES

1. Terner, J.; Spiro, T.G.; Nagumo, M.; Nicol, M.F.; El-Sayed, M.A. J. Am. Chem. Soc., 102, 3238 (1980). Caswell, D.S.; Spiro, T.G. J. Am. Chem. Soc., 109, 2796 (1987). Teraoka, J.; Harmon, P.A.; Asher, S.A. App. Spectroscopy 1988, submitted.
2. Simpson, S.F.; Kincaid, J.R.; Holler, J.F. J. Am. Chem., 58, 3136 (1986).
3. Oertling, W.A. and Babcock, G.T. J. Am. Chem. Soc., 107, 6406 (1985).
4. Varotsis, C.; Woodruff, W.H.; Babcock, G.T. J. Am. Chem. Soc., 111, 6439 (1989); 112, 1297 (1990).
4. Ogura, T.; Hon-nami, K.; Oshima, T.; Yoshikawa, S.; Kitagawa, T. J. Am. Chem. Soc., 105, 7781 (1983).
5. Salmeen, I.; Rimai, L.; Babcock, G.T. Biochemistry, 17, 800 (1978).

CHAPTER 3

TIME-RESOLVED RAMAN DETECTION OF ν(FE-O) IN AN EARLY INTERMEDIATE IN THE REDUCTION OF O_2 BY CYTOCHROME OXIDASE*

SUMMARY

Flash photolysis of carbon monoxy cytochrome oxidase subsequent to its rapid mixing with oxygenated buffer has been used to initiate the reduction of O_2 by the enzyme. By delaying a second laser pulse relative to the photolysis pulse, time resolved resonance Raman spectra have been recorded during the reaction. In the spectrum recorded at 10 μs after CO photolysis, a mode is observed at 571 cm^{-1} that shifts to 546 cm^{-1} when the experiment is repeated with $^{18}O_2$. The appearance of this mode is dependent upon the laser intensity used and it disappears at higher incident energies. We assign this mode to the Fe-O stretching vibration of an early O_2 adduct in the cytochrome oxidase/dioxygen reaction. Consideration of recent data on

---

*Varotsis, C.; Woodruff, W. H.; and Babcock, G. T., J. Am. Chem. Soc., 111, 6439-6440 (1989); 112, 1297 (1990).

dioxygen adducts of other heme proteins and model hemes indicates that this early intermediate is most likely the cytochrome a_3^{2+}-O_2 complex.

Cytochrome oxidase contains four redox active centers per functional unit: cytochromes a and a_3 and the copper atoms, Cu_A and Cu_B. Cytochrome c, the physiological substrate of cytochrome oxidase, transfers electrons to the cyt_a and Cu_A sites. These reducing equivalents are transferred to the binuclear $cyt_{a_3}...Cu_B$ center, which binds O_2 and reduces it to H_2O. Although the reaction between O_2 and cytochrome oxidase occurs too quickly to be studied by conventional stopped-flow techniques, Gibson and Greenwood[1] showed that photolysis of the cytochrome a_3^{2+}-CO complex of the enzyme in the presence of O_2 could be used to circumvent this limitation. Babcock et al.[2,3] adopted this approach and used time-resolved resonance Raman to study the reaction of fully- and partially-reduced cytochrome oxidase with O_2. Although instrumental limitations restricted data acquisition to the high frequency (>1000 cm^{-1}) range, they concluded that the reoxidation of cytochrome oxidase proceeds via a cytochrome a_3^{2+}-O_2 complex that resembles oxymyoglobin and oxyhemoglobin. Direct detection of iron/bound oxygen ligand vibrations is necessary to test these conclusions as well as to provide detailed information on subsequent intermediates in the dioxygen reduction reaction. To this end, we have developed techniques that allow us to carry

out low-frequency Raman detection under flow/flash conditions; here we report ν(Fe-O) for an early intermediate in the cytochrome oxidase/dioxygen reaction. Consideration of data on dioxygen adducts of other heme proteins and model hemes indicates that this early intermediate is most likely the cytochrome a_3-O_2 complex.

Cytochrome oxidase was prepared from beef hearts according to a modified Hartzell and Beinert procedure and dissolved in 50 mM HEPES, 0.5% lauryl maltoside, pH 7.4. The fully-reduced, carbon monoxide-bound enzyme is prepared by anaerobic reduction with 4mM sodium ascorbase and 1 μM cytochrome c under CO. The absorption spectrum of the enzyme-CO complex (inset Figure 3.2) shows a Soret maximum at 430 nm, as expected.[4] The enzyme solution and the O_2 saturated buffer solution are placed in separated syringes and driven through two eight-jet mixers in series at flow rates of 0.4 ml/min by using a DSAGE 355 syringe pump. The syringe pump drive is set so that 2.5 changes of sample occurred in the scattering volume for each pump-probe pair. The exit port of the mixer is designed to allow the oxidase solution to form a free jet in air in the scattering volume, which eliminates quartz scattering. The reaction starts when the mixed solution comes into the laser beam. Photodissociation of carbon monoxide from $a^{2+}a^{2}{}_{3}{}^{+}$. CO is followed by the reaction of $a^{2+}a^{2}{}_{3}{}^{+}$ with O_2. The spectrum arises from intermediates which are produced while the photodissociated enzyme stays in the laser beam.

The time-resolved resonance Raman experiment employs two Quanta Ray, pulsed lasers with pulse widths of 10 ns and repetition rates of 10 Hz and a digital delay generator which provides programmable triggering for the flash lamps and Q-switches (Figure 3.1). This delay is continuously monitored with a photodiode to collect scattering laser light from a glass slide mounted in front of the sample and a Tektronix oscilloscope to observe the delay. The pump pulse from the first laser (532 nm, 1.3 mJ) is sufficient to dissociate the CO and initiate the oxidase/oxygen reaction. The probe wavelength (427 nm) is provided by pumping stilbene 420 with the third harmonic output (355 nm) of the second laser. The scattered radiation is collected with a SPEX 1459 Illuminator, dispersed in a SPEX 1877 Triplemate, and detected by an EG&G PARC 1420 diode array detector.

Time-resolved resonance Raman spectra of cytochrome oxidase at 10 μs subsequent to carbon monoxide photolysis in the presence of O_2 are shown in Figure 3.2A-D. Spectrum E is that of the photodissociation product of the reduced carbonmonoxy enzyme (pump-probe delay = 10 ns.). Spectrum A, obtained with a low energy, defocused beam (0.3 mJ), is similar to the 10 ns spectrum with the exception that a new mode appears at 571 cm^{-1}. Figure 3.2B shows that the 571 cm^{-1} mode in the $^{16}O_2$ spectrum is downshifted to 546 cm^{-1} mode when the experiment is repeated with $^{18}O_2$. This allows us to assign it as an Fe-O stretching motion in the

Figure 3.1 Instrumental configuration used for pulsed, time-resolved resonance Raman measurements of flowing cytochrome oxidase samples prepared by rapid mixing.

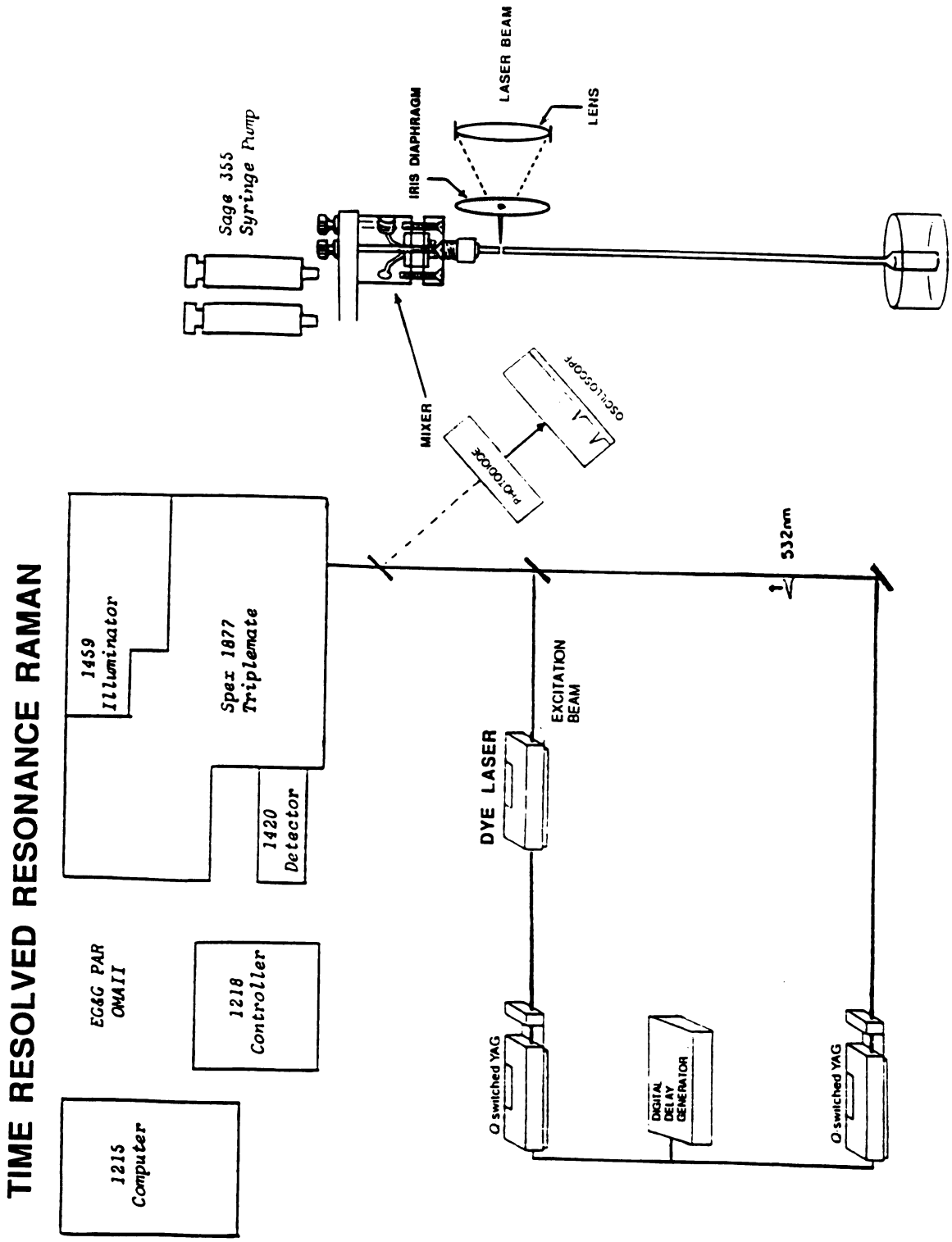
TIME RESOLVED RESONANCE RAMAN
1215 Computer
EG&G PAR OMA II
1218 Controller
1459 Illuminator
Spex 1877 Triplemate
1420 Detector
DYE LASER
EXCITATION BEAM
532nm
Q switched YAG
DIGITAL DELAY GENERATOR
Q switched YAG
MIXER
PHOTODIODE
OSCILLOSCOPE
Sage 355 Syringe Pump
IRIS DIAPHRAGM
LASER BEAM
LENS

Figure 3.2 Time-resolved resonance Raman spectra of cytochrome oxidase following initiation of the reaction with oxygen at room temperature. The energy of the 532 nm photolysis pump pulse was 1.3 mJ, sufficient to photolyze the enzyme·CO complex and initiate the O_2 reduction reaction. The energy of the probe beam was 0.3 mJ for spectra A and B[14] and 1.0 mJ for spectra C-E. The repetition rate for both the pump and probe pulses (10 ns duration) was 10 Hz. The pump-probe delay was 10 μs for the spectra A-D and 10 ns for the transient spectrum E. The accumulation time was 110 min for spectrum A, 70 min for spectrum B, 5 min for spectra C and D, and 15 min for spectrum E.

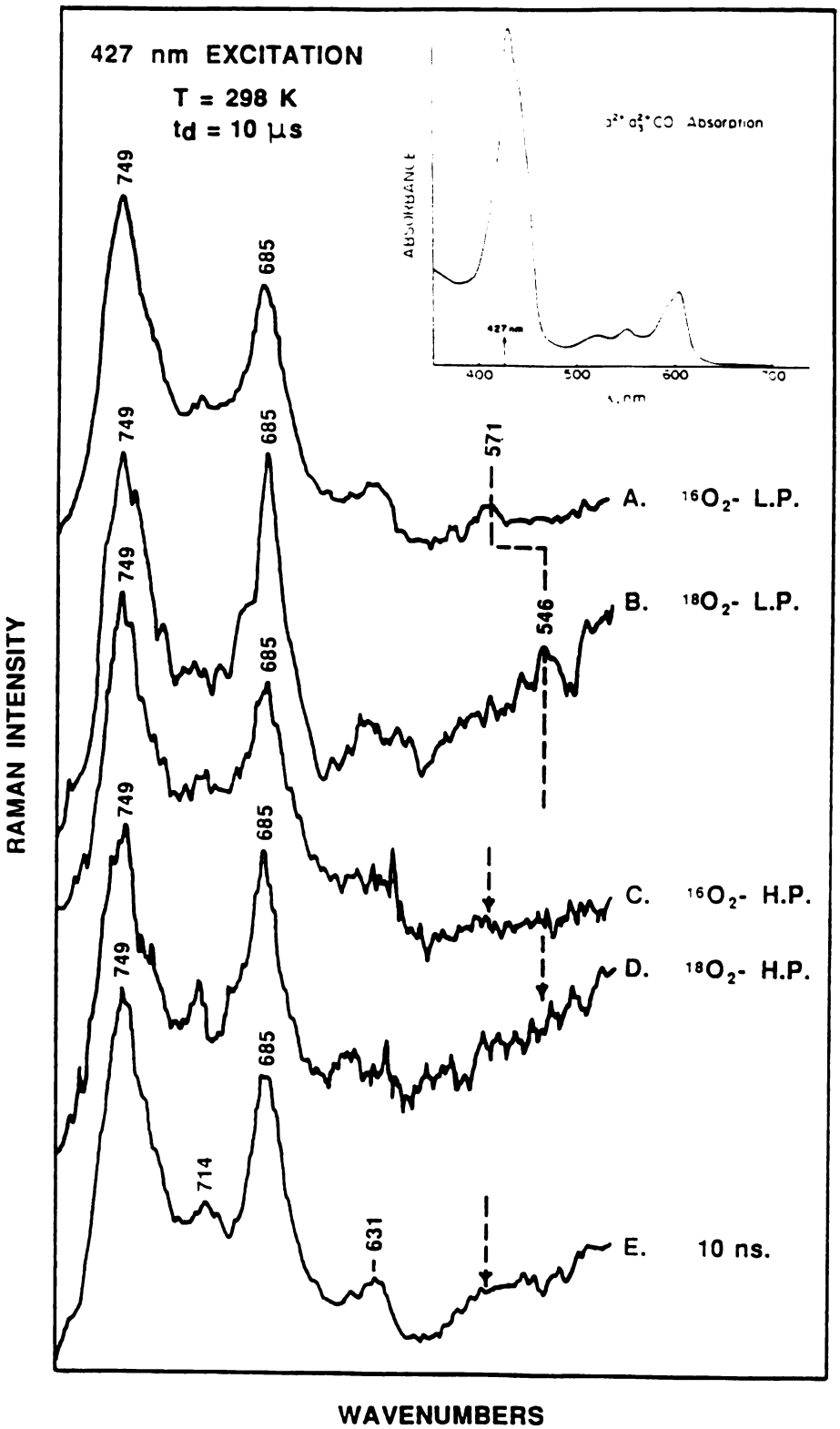
427 nm EXCITATION
T = 298 K
td = 10 μs
749
685
571
546
631
714
A. $^{16}O_2$- L.P.
B. $^{18}O_2$- L.P.
C. $^{16}O_2$- H.P.
D. $^{18}O_2$- H.P.
E. 10 ns.
RAMAN INTENSITY
WAVENUMBERS
400
500
600
427 nm

cytochrome a_3/O_2 complex, as the 25 cm^{-1} shift is in agreement with that expected from the two-body harmonic oscillator approximation for $Fe-O_2$. Spectra C and D were obtained with relatively high energies (1mJ) and the absence of any modes located at 571 cm^{-1} (Figure 3.2C, $^{16}O_2$) and 546 cm^{-1} (Figure 3.2D, $^{18}O_2$) indicates photodissociation of the oxy ligand, as was observed in the high frequency experiments,[2,5] and further supports our assignment of the 571 cm^{-1} mode in the cytochrome oxidase/O_2 complex.

The most reasonable assignment of the 571 cm^{-1} mode is that it arises from a cytochrome $a_3{}^{2+}-O_2$ complex. Such an assignment is consistent with the photolability of this species,[2b] but more important, it is in reasonable agreement with $\nu(Fe^{2+}-O_2)$ frequencies observed in other heme $Fe^{2+}-O_2$ complexes. Table 3.1 summarizes several of these frequencies; the 571 cm^{-1} mode for the oxidase intermediate is similar to $\nu(Fe^{2+}-O_2)$ for several dioxygen-bound heme species. Several further points can be made from the Table 3.1. First, the $\nu(Fe-O_2)$ in the oxidase intermediate is 5 cm^{-1} lower than that of the imidazole-heme a $Fe^{2+}-O_2$ complex, despite the fact that the model compound reproduces the immediate coordination sphere that is expected to occur around the iron in the protein environment. We do not regard this decrease as mechanistically significant, as discussed below. Second, the oxidase species has a frequency that is close to the

Table 3.1

Vibrational frequencies for dioxygen bound complexes.

	ν(Fe-O)	ref
Cytochrome Oxidase	571	this work
Hb	567	11
Mb	570	9
HRP III	562	9
Im (heme a) Fe^{2+}-O_2	576	7
(TMP)-Fe-O-O-Fe(TMP)	574	6
(Pip)(TPP)Fe^{2+}-O_2	575	12
(TPP)Fe^{2+}-O_2	509	12

Abbreviations:

Hb, hemoglobin
Mb, myoglobin
HRP, horseradish Peroxidase
Im, imidazole
Pip, piperazine
TPP, meso-tetraphenyl porphyrin

574 cm^{-1} observed for the iron-oxygen stretching frequency for the five coordinate μ-peroxo dimer reported by Nakamoto and co-workers.[6] Despite the similarity in those two frequencies, we nevertheless favor a cyt a_3^{2+}-O_2 structure for the intermediate we detect. The basis for this lies in our expectation that cytochrome a_3 will retain its proximal histidine ligand during catalysis and thus that a peroxy a_3 species will have ν(Fe-O) at significantly higher frequencies than the five coordinate model compound.[7] A similar frequency increase in the iron-oxygen stretching frequency is apparent in Table 3.1 when one compares the five-coordinate (TPP)Fe^{2+}-O_2 complex (ν(Fe-O)=509 cm^{-1}) to the six-coordinate (Pip)(TPP)Fe^{2+}-O_2 species (ν(Fe-O)=575 cm^{-1}) and is also apparent in heme ferryl oxo species.[7].

The $\nu(Fe^{2+}$-O) frequency at 571 cm^{-1} indicates that the cytochrome a_3-O_2 complex is unperturbed by distal effects in the cytochrome a_3/Cu_B binding site. Weakening and rupture of the O=O bond[2a,8,13] occurs subsequent to formation of the initial dioxygen-a_3^{2+} adduct.

REFERENCES

1. a) Gibson, Q; Greenwood, C. Biochem. J. 1963, 86, 541. b) Greenwood, C.; Gibson, Q. J. Biol. Chem. 1967, 242, 1782. c) Greenwood, C.; Hill, B. Biochim. J. 1984, 218, 913. d) Hill, B.; Greenwood C.; Nichols, P. Biochim. Biophys. Acta 1986, 853, 91. e) This technique has been modified for low temperature application by Chance and co-workers and has been used to study the oxidase/O_2 reaction in frozen samples by several groups. See: Chance, B.; Saronio, C.; Leigh, J. S. J. Biol. Chem. 1975, 250, 9226. Clore, G. M.; Andreasson, L. E.; Karlsson, B.; Aasa, R.; and Malmstrom, B. G. Biochem J. 1980, 185, 139. Chan, S. I.; Witt, S. N.; Blair, D. F. Chemica Scripta 1988, 28A, 51. For review, see Naqui A. and Chance B. Ann. Rev. Biochem. 1986, 55, 137.
2. a) Babcock, G.T.; Jean, J. M.; Johnston, L. N.; Palmer, G.; Woodruff, W. H. J. Am. Chem. Soc. 1984, 106, 8305. b) Babcock, G. T.; Jean, J. M.; Johnston, L. N.; Woodruff, W. H.; Palmer, G. J. Inorg. Biochem., 1985, 23, 243.
3. Babcock, G. T. "Biological Applications of Raman Scattering", Spiro, T.G., ed., 1988, Vol. 3, 295.
4. Vanneste, W. H. Biochem. 1966, 5, 838.
5. Varotsis, C. and Babcock, G.T., unpublished results.
6. Paeng, I.R.; Shiwaku, H.; Nakamoto, K. J. Am. Chem. Soc. 1988 110, 1995.

7. Oertling, W.A.; Kean, R. T.; Wever, R.; Babcock, G.T. Inorg. Chem., 1990, in press.

8. Blair, D.F.; Witt, S.N.; Chan, S.I. J. Am. Chem. Soc., 1985, 107, 7389.

9. Van Wart, H.; Zimmer, J. J. Biol. Chem. 1985, 250, 8372.

10. M. Wikstrom, K. Krab and M. Saraste, "Cytochrome Oxidase, A Synthesis", Acad. Press, New York, 1981.

11. Brunner, H. Naturwissenschaften 1974, 61, 129.

12. Nakamoto, K.; Paeng, I. R.; Kuroi, T.; Iosbe, T.; Oshio, H. J. Mol. Structure 1988, 189, 293.

13. Wikstrom, M. Proc. Nat. Acad. Sci. USA 1981, 78, 4051.

14. A loose point focus at the sample was used to decrease the probe power density. We estimate that the probe power density used to record spectra A and B was 12-fold less than in spectra C-E.

CHAPTER 4

DIRECT DETECTION OF A DIOXYGEN ADDUCT OF CYTOCHROME A_3 IN THE MIXED VALENCE CYTOCHROME OXIDASE/DIOXYGEN REACTION*

SUMMARY

Time-resolved resonance Raman spectra have been recorded during the reaction of mixed valence ($a^{3+}a_3^{2+}$) cytochrome oxidase with dioxygen at room temperature. In the spectrum recorded at 10 μs subsequent to carbon monoxide photolysis a mode is observed at 572 cm^{-1} that shifts to 548 cm^{-1} when the experiment is repeated with $^{18}O_2$. The appearance of this mode is dependent upon the laser intensity used and it disappears at higher incident energies. The high frequency data, in conjunction with the mid-frequency data, allow us to assign the 572 cm^{-1} mode to the Fe-O stretching vibration of the low-spin O_2 adduct that forms in the mixed valence cytochrome oxidase/dioxygen

---

*Varotsis, C.; Woodruff, W. H.; and Babcock, G. T., 1990, J. Biol. Chem., in press.

reaction. The 572 cm^{-1} $\nu(Fe-O_2)$ frequency in the mixed valence/O_2 adduct is essentially identical to the 571 cm^{-1} frequency we measured for this mode during the reduction of O_2 by the fully reduced enzyme (Varotsis, C., Woodruff, W.H. and Babcock, G.T. J. Am. Chem. Soc., **111**, 6439-6440 (1989), **112**, 1297, (1990)), which indicates that the O_2-bound cytochrome a_3 site is independent of the redox state of the cytochrome a/Cu_A pair. The photolabile oxy intermediate is replaced by photostable low- or intermediate-spin cytochrome $a_3{}^{3+}$ with $t_{½} \simeq 200$ μs.

INTRODUCTION

Cytochrome oxidase, the terminal enzyme complex of the mitochondrial respiratory chain, catalyzes the transfer of electrons from reduced cytochrome c to molecular oxygen. Four electrons are funnelled into O_2 in this reaction to reduce it to H_2O; concomitantly, the free energy made available in the electron transfer reactions that occur during O_2 reduction is used to pump protons from the matrix to the cytosolic side of the inner mitochondrial membrane. The free energy stored in the proton gradient is used ultimately to drive adenosine triphosphate formation(1). The enzyme isolated from bovine heart contains two hemes, cytochrome a and a_3, two associated copper atoms, Cu_A and Cu_B, magnesium and zinc(2,3). The cytochromes and copper atoms are redox active, but the roles of the other metals, if any, remain uncertain. The complex, intramolecular

electron transfers that occur between cytochrome a/Cu_A and the binuclear center cytochrome a_3/Cu_B, where the four-electron reduction of molecular oxygen to water occurs, have been studied by various spectroscopic techniques(4-23). The focus in this work has been on characterizing intermediates that occur in dioxygen reduction, which is essential for elucidating the chemical mechanism of the redox processes catalyzed by the enzyme.

Although the reaction between cytochrome oxidase and O_2 occurs too quickly ($t_{½}$ = 1 ms) to be studied by conventional stopped flow techniques, Gibson and Greenwood(4) used photolysis of the cytochrome $a_3^{2+}\cdot CO$ complex of the enzyme in the presence of O_2 to circumvent this limitation. Hill and Greenwood(8) showed that by starting from the mixed valence state in which only cytochrome a_3 and Cu_B are reduced, partially reduced oxygen species were generated as intermediates on a microsecond-to-millisecond time scale at room temperature. Chance et al.(9) developed techniques to study the reaction on a second-to-minute time scale at low temperatures. With this approach, Chance and coworkers(9), Clore et al.(10), Chan et al.(11,12) and Denis(13) studied intermediates involved in dioxygen reduction and characterized them by using optical and EPR spectroscopies. The intermediate species formed in the reaction of the enzyme with O_2 at room temperature are, however, not yet well defined, although a variety of structures have been postulated (e.g. 1, 9, 10-

12, 15, 16, 19, 21, 22). Time-resolved resonance Raman spectroscopy provides the unique possibility of detecting out-of-plane ligand vibrational modes and thus the structure of the bound dioxygen species through isotopic labeling of the O_2. Moreover, information concerning heme geometric and electronic properties is accessible. Monitoring the time evolution of these species provides the opportunity to explore the dioxygen reduction mechanism in detail.

Babcock et al.(18,19) adapted the Gibson/Greenwood technique and used time-resolved resonance Raman to study the reaction of fully and partially reduced oxidase with O_2. Although instrumental limitations restricted data acquisition to the high frequency (>1200 cm^{-1}) region, they concluded that photolabile oxy species were the initial intermediates in both reactions. They postulated that these dioxygen adducts were replaced by non-photolabile species in which cytochrome a_3 was oxidized with $t_{1/2}$ = 60 μs and 200 μs in the fully reduced and mixed valence complexes, respectively. Ogura et al.(20,21) applied continuous wave, one laser Raman techniques and reported transient resonance Raman spectra of intermediates formed within 100 μs after photolysis of the fully reduced CO complex. Neither of these studies reported direct detection of the iron/bound oxygen ligand vibration.

More recently, observation of oxygen isotope sensitive ligand vibrations have been reported. Rousseau et al.(22)

observed a mode at 477 cm^{-1} under intense laser illumination, which they attributed to Fe^{3+}-OH^- motion in a cytochrome a_3/hydroxide adduct. Owing to uncertainties as to the physiological relevance of the experimental protocol, however, the catalytic significance of this species is unclear. In our own work (Varotsis et al., 1989), we have extended the flow/flash time-resolved approach so as to be able to observe the low frequency region of the Raman spectrum at early times in the O_2/reduced cytochrome oxidase reaction. In our initial work, we observed an isotope sensitive mode at 571 cm^{-1} at 10 μs into the reduction reaction that we assigned to $\nu(Fe^{2+}-O_2)$ in the initial reduced cytochrome oxidase/dioxygen adduct.

In the experiments reported here, we have applied our flow/flash, time-resolved Raman approach to study the reaction between mixed valence cytochrome oxidase and dioxygen. The use of this complex allows us to obtain further insight into the reaction of cytochrome oxidase with O_2 at room temperature; the interaction of this species with O_2 also serves as a benchmark for studies in which partially reduced oxygen species, such as hydrogen peroxide or superoxide, are added to the enzyme. Finally, it provides us with information as to whether the low temperature oxygenated species(9-14) are populated at room temperature. Our results indicate that the dioxygen adduct of cytochrome $a_3{}^{2+}$ is formed in the mixed valence enzyme

and that the redox states of cytochrome a and of Cu_A do not influence the vibrational characteristics of this species.

EXPERIMENTAL PROCEDURES

Cytochrome oxidase was prepared from beef hearts by using a modified Hartzell-Beinert preparation(24) and was frozen under liquid N_2 until ready for use. The enzyme was solubilized in 50 mM HEPES (4-(2-hydroxyethyl)-1-piperazineethanesulfonic acid) at pH 7.4 with 0.5% dodecyl β-D-maltoside. The mixed valence/CO enzyme was prepared by exposing an anaerobic solution of the resting enzyme to carbon monoxide for five hours(8). The absorption spectrum of the mixed valence·CO complex (inset, Fig. 3) shows a Soret maximum at 430 nm as expected(25). The enzyme solution and an oxygen saturated buffer solution (50 mM HEPES, 0.5% dodecyl β-D-maltoside, pH 7.4, 1.2 mM [O_2]) were placed in separate syringes and driven through two eight-jet tangential Gibson type mixers in series at a flow rate of 0.4 ml/min with a SAGE 355 syringe pump. The syringe pump drive was set so that 2.5 changes of sample occurred in the scattering volume for each pump-probe pulse pair. The exit port of the mixer is designed to allow the oxidase solution (40 μM after mixing) to form a free jet in air in the scattering volume, which eliminates quartz scattering(26). The reaction is initiated when the mixed valence·CO/O_2 solution comes into the scattering volume. Photodissociation of carbon monoxide from $a^{3+}a_3{}^{2+}$·CO is

followed by reaction of $a^{3+}a_3^{2+}$ with oxygen. In the time-resolved resonance Raman experiment, two Quanta Ray DCR 2A pulsed lasers with pulse widths of 10 ns and repetition rates of 10 Hz were used. A digital delay generator (Stanford Research Systems, Inc., Model DG 535) provided programmable triggers for the flash lamps and Q-switches. The pump pulse from the first laser (532 nm, 1.3 mJ) was sufficient to dissociate CO and initiate the oxidase/oxygen reaction. The probe wavelength (427 nm) was provided by pumping stilbene 420 with the third harmonic output (355 nm) of the second laser. The scattered radiation was collected with a SPEX 1459 Illuminator, dispersed in a SPEX 1877 Triplemate, and detected by an EG&G PAR 1420 diode array detector. A linear sloping background was subtracted from the resonance Raman spectra in Figure 3 and Figure 4, but no smoothing was done. Optical absorption spectra were obtained with a Perkin-Elmer Lamda 5 uv-visible spectrophotometer.

RESULTS

In Figure 1 (B-F) we present high frequency time-resolved resonance Raman spectra of mixed valence ($a^{3+}a^{2+}$) cytochrome oxidase at various delay times (10 μs - 500 μs) subsequent to carbon monoxide photolysis in the presence of O_2. These spectra, as well as those of the 10 ns photoproduct (Fig. 1A) and resting enzyme (Fig. 1G), were recorded with ~1 mJ/pulse. With 427 nm excitation, the

Figure 4.1 Time-resolved resonance Raman spectra of mixed valence cytochrome oxidase at the indicated times following initiation of the reaction with oxygen at room temperature. The energy of the 532 nm photolysis pump pulse was 1.3 mJ, sufficient to photolyze the enzyme -CO complex and initiate the O_2 reduction reaction. The energy of the probe beam was 1.0 mJ for all spectra. The spectrum of the resting enzyme was obtained by using the probe beam only. The repetition rate for both the pump and probe pulses (10 ns duration) was 10 Hz. The accumulation time was 15 min. for each spectrum.

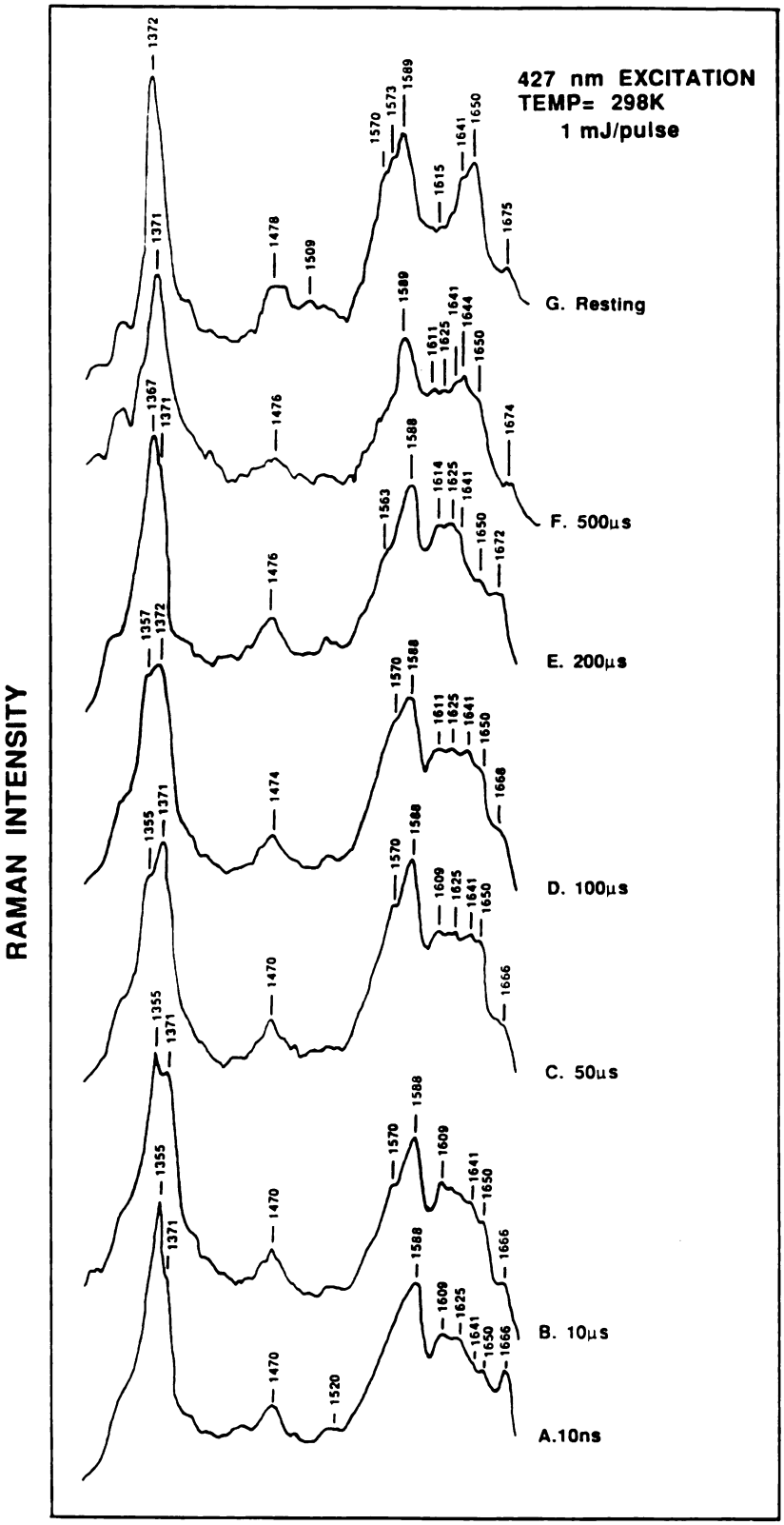
427 nm EXCITATION
TEMP= 298K
1 mJ/pulse
G. Resting
F. 500µs
E. 200µs
D. 100µs
C. 50µs
B. 10µs
A.10ns
RAMAN INTENSITY
WAVENUMBERS

contribution of cytochrome a to the resonance Raman spectrum of resting enzyme is emphasized because of the relative positions of the Soret maxima of cytochrome a at 427 nm and cytochrome a_3 at 414 nm(27-29). In the spectrum of the resting enzyme (Fig. 1G) the oxidation state marker is at 1372 cm^{-1}, establishing that both cytochromes are in the ferric (Fe^{3+}) state. The core expansion region shows two vibrations at 1573 cm^{-1} (high-spin cyt a_3^{3+}) and 1589 cm^{-1} (low-spin cyt a^{3+}). The 1615 cm^{-1} and 1641 cm^{-1} modes arise from ν_{10} of a_3^{3+} and a^{3+}, respectively. The 1650 cm^{-1} and 1675 cm^{-1} have been assigned(17,27) as the C=O stretching vibration of the formyl groups (-CHO) of a^{3+} and a_3^{3+}, respectively.

The most notable changes that occur in the evolution from the photoproduct spectrum (A, 10 ns) to the oxidase/O_2 transient spectra (B-F, 10 μs - 500 μs) are as follows. (1) The porphyrin π^* electron density sensitive mode, ν_4, of cytochrome a_3^{2+}, which is located at 1355 cm^{-1} in the photoproduct spectrum, displays intensity and/or position changes, while ν_4 of cytochrome a at 1371 cm^{-1} remains essentially as a spectator during the oxidation process. Little change in the 1355 cm^{-1} position of ν_4 (a_3^{2+}) is apparent in the 10, 50 and 100 μs spectra but at 200 μs (spectrum E) ν_4 appears at 1367 cm^{-1}. At 500 μs following initiation of the reaction the oxidation state marker has shifted to 1371 cm^{-1}, which indicates essentially complete generation of a non-photolabile form of the enzyme in which

Figure 4.2 Time-resolved resonance Raman spectra of mixed valence cytochrome oxidase following initiation of the reaction with oxygen at room temperature. The pump-probe delay was 10 μs for spectra A and C and 2 μs for spectrum B. The energy of the probe beam was 0.3 mJ for spectra B and C and 1.0 mJ for spectrum A. The accumulation time was 45 min. for spectra B and C and 15 min. for spectrum A.

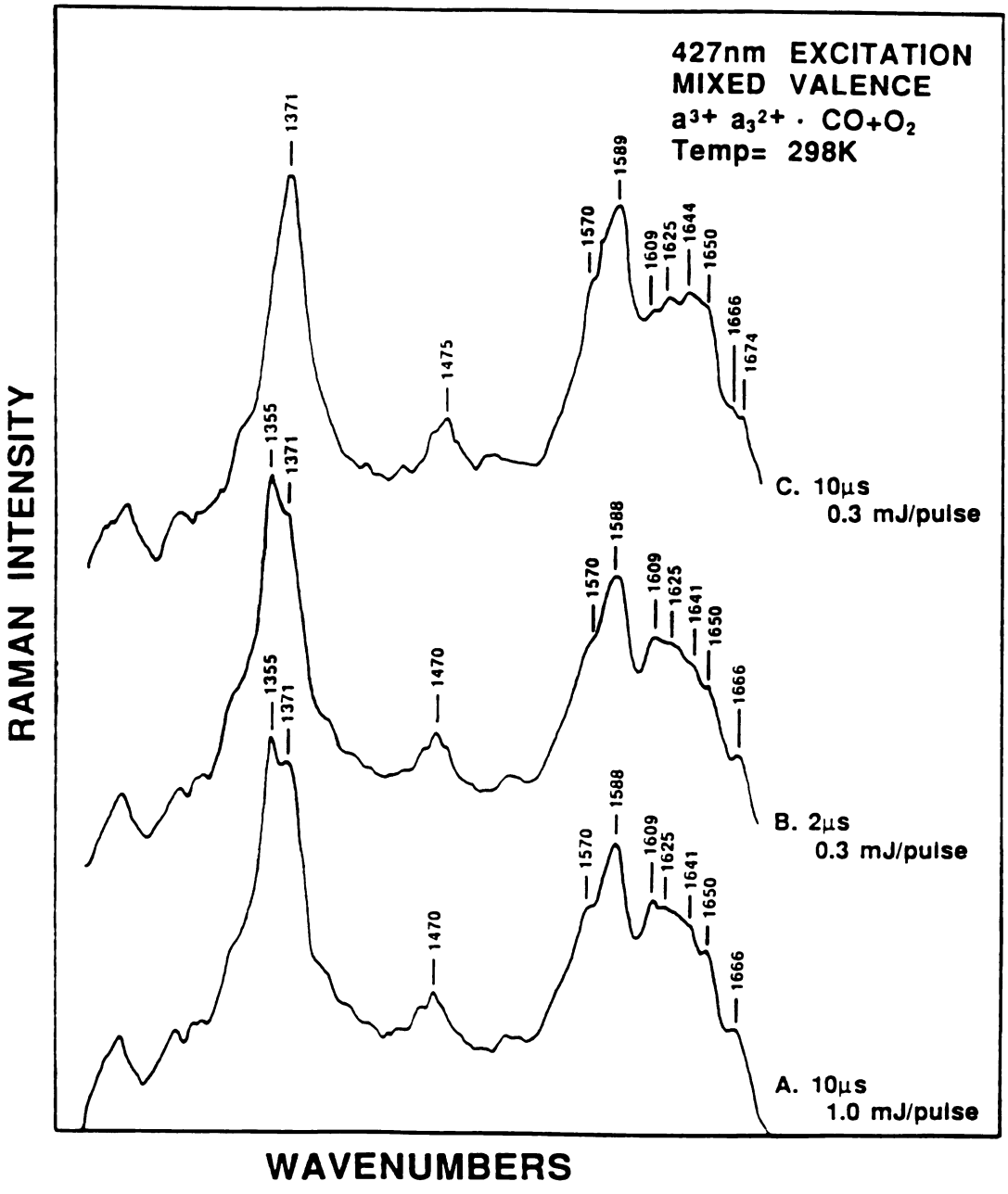
427nm EXCITATION
MIXED VALENCE
a^{3+} a_3^{2+} · CO+O_2
Temp= 298K
1371
1589
1570
1609
1625
1644
1650
1666
1674
1475
C. 10μs
0.3 mJ/pulse
1355
1371
1588
1570
1609
1625
1641
1650
1666
1470
B. 2μs
0.3 mJ/pulse
1355
1371
1588
1570
1609
1625
1641
1650
1666
1470
A. 10μs
1.0 mJ/pulse
RAMAN INTENSITY
WAVENUMBERS

cytochrome a_3 has been oxidized. (2) The cytochrome a_3 core-size sensitive band, ν_2, which appears at 1570 cm^{-1} at delay times less than 100 μs, shifts to higher frequency and moves underneath the ν_2 low spin vibration of cytochrome a^{3+} at 1588 cm^{-1} in the 200 and 500 μs time delay spectra. The shift in this mode, along with the ν_4 shift noted above, shows that cytochrome a_3, which is oxidized at 500 μs in the reaction, is in either a low- or intermediate-spin state(19,30). (3) The vinyl stretching mode at 1625 cm^{-1} seems to be insensitive to the oxidation state or spin state of the iron of cytochrome a_3. (4) The ν_{10} vibration at 1611 cm^{-1} in the 500 μs spectrum has lost intensity and is slightly upshifted from its original position at 1609 cm^{-1} in the photoproduct spectrum. Ching et al.(31) reported a decrease in intensity of this mode upon CN^- binding to cytochrome a_3 and Rousseau et al.(32) observed similar behavior upon NO binding, indicating that this mode is sensitive to the ligation state of the cytochrome a_3 site. (5) The cytochrome a_3 formyl stretching vibration, located at 1666 cm^{-1} in the 10 ns spectrum, has lost intensity in the 10, 50 and 100 μs spectra and has shifted to 1672 cm^{-1} and 1674 cm^{-1} in the 200 μs and 500 μs spectra, respectively.

Figure 2 shows Raman spectra recorded at 2 μs and 10 μs following the reaction between mixed valence cytochrome oxidase and dioxygen. Spectrum A (t_d = 10 μs) was obtained with relatively high energy laser pulses (1 mJ), while

Figure 4.3 Time-resolved resonance Raman spectra of mixed valence cytochrome oxidase following initiation of the reaction with oxygen at room temperature. The energy of the 532 nm photolysis pump pulse was 1.3 mJ. The energy of the probe beam was 0.3 mJ for spectra A and B and 1.0 mJ for spectra C, D, and E. The repetition rate for both the pump and probe pulses (10 ns duration) was 10 Hz. The pump-probe delay was 10 μs for the spectra A-D and 10 ns for the transient spectrum E. The accumulation time was 120 min. for spectrum A, 65 min. for spectrum B, 5 min. for spectra C and D and 15 min. for spectrum E.

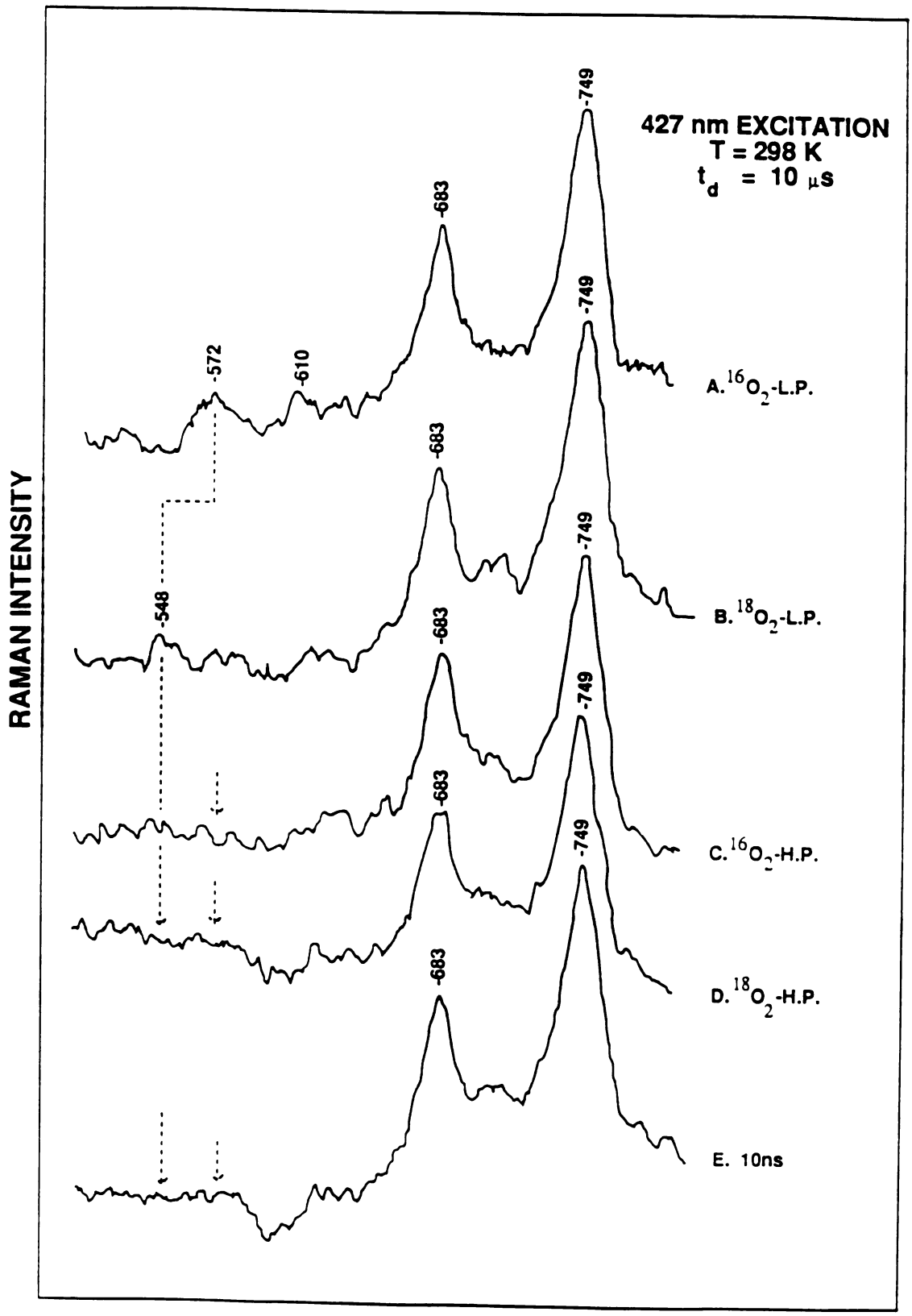
427 nm EXCITATION
T = 298 K
t_d = 10 μs
-749
-683
-572
-610
A. $^{16}O_2$-L.P.
-548
B. $^{18}O_2$-L.P.
C. $^{16}O_2$-H.P.
D. $^{18}O_2$-H.P.
E. 10ns
RAMAN INTENSITY
WAVENUMBERS

spectra B and C were obtained with a low energy, defocused beam (0.3 mJ) to avoid photolysis of the cytochrome a_3/O_2 species previously postulated from high frequency Raman data(18,19). We expect that cytochrome a^{3+} and the postulated cytochrome $a_3{}^{2+}/O_2$ adduct will contribute comparable intensities to the resonance Raman spectra as each should exhibit an absorbance maximum at 427 nm. The marked differences we observe in the 10 μs spectra as a function of laser power (Fig 2A and C) confirm the initial occurrence of a photolabile species. The higher energy spectrum is essentially unchanged relative to the photoproduct spectrum in Figure 1 and the low power, 2 μs spectrum in Figure 2B. At lower energy, however, Figure 2C shows that the oxidation state marker has shifted to 1371 cm^{-1} and the shoulder at 1356 cm^{-1} is substantially decreased at 10 μs relative to the 2 μs spectrum. In the spin marker region, the 1570 cm^{-1} mode has lost intensity, whereas the 1589 cm^{-1} mode has increased in intensity. The carbonyl stretching mode of the formyl group in cytochrome a_3 exhibits two vibrations at 1666 and 1674 cm^{-1}.

The data in Figures 1 and 2 confirm and extend earlier, time-resolved Raman data on the mixed valence cytochrome oxidase/dioxygen reaction(19). In particular, they show that a photolabile intermediate is formed in the early stages of the reaction and that this species persists for ~200 μs following its formation. In the earlier Raman work, as well as in flow/flash, time-resolved optical

Figure 4.4 Difference spectra of the initial intermediate in the reaction of mixed valence cytochrome oxidase with isotopes of oxygen observed at 10 μs into the reaction. Spectrum A was obtained by subtracting the low power $^{18}O_2$ spectrum (Figure 3B) from the low power $^{16}O_2$ spectrum (Figure 3A). Spectrum B was obtained by subtracting the high power $^{16}O_2$ (Figure 3C) spectrum from the low power $^{16}O_2$ spectrum (Figure 3A).

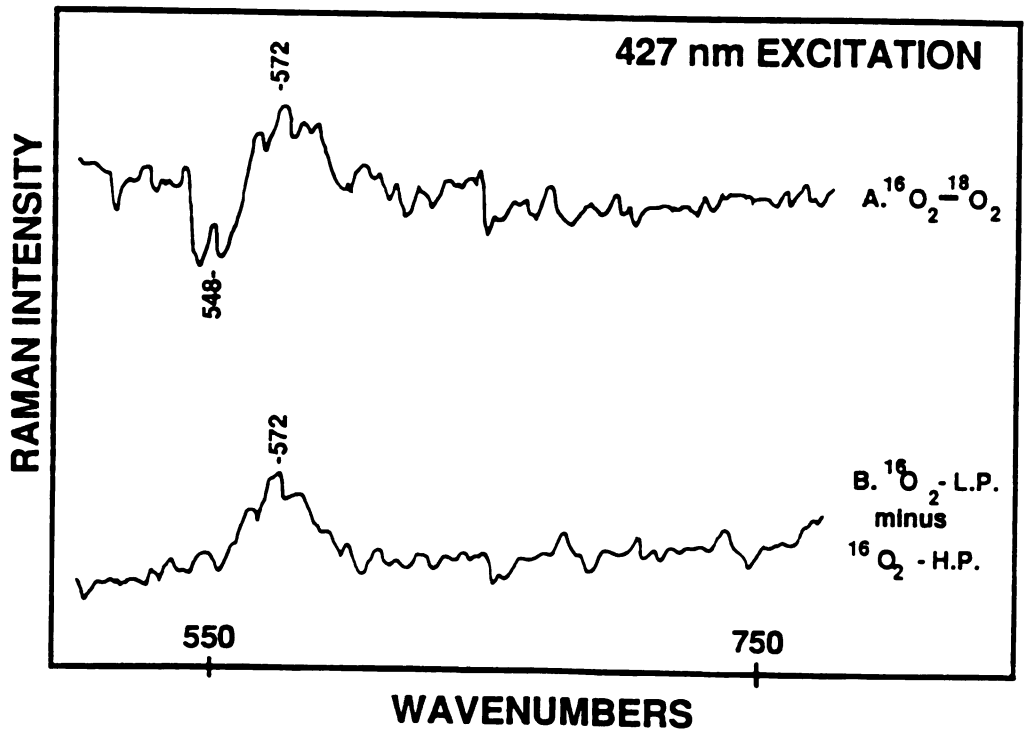
427 nm EXCITATION
-572
548-
A. $^{16}O_2$–$^{18}O_2$
-572
B. $^{16}O_2$ - L.P.
minus
$^{16}O_2$ - H.P.
RAMAN INTENSITY
550
750
WAVENUMBERS

work(8,16), this species was assigned as a cytochrome a_3^{2+}/dioxygen adduct. Direct confirmation of this hypothesis requires detection of the Fe a_3^{2+} - O_2 stretching vibration.

The mid-frequency spectra at 10 μs subsequent to carbon monoxide photolysis in the presence of O_2 are shown in Figure 3(A-D). Spectrum E is that of the photodissociation product of the mixed valence carbon monoxy enzyme (pump-probe delay = 10 ns). Spectrum A was obtained with a low energy, defocused beam (0.3 mJ) and is similar to the 10 ns spectrum with the exception that a new mode appears at 572 cm^{-1}. Figure 3B shows that the 572 cm^{-1} mode in the $^{16}O_2$ spectrum is downshifted to 548 cm^{-1} when the experiment is repeated with $^{18}O_2$. This allows us to assign it as the iron-oxygen stretching vibration in the $a^{3+}a_3^{2+}$-O_2 complex, as the 24 cm^{-1} shift is in agreement with that expected from the two-body harmonic oscillator approximation for Fe^{2+}-O_2. Spectra C and D were obtained with relatively high energy (1 mJ) laser pulses and the absence of modes located at 572 cm^{-1} (Figure 3C) and 548 cm^{-1} (Figure 3D) indicates photodissociation of the oxy ligand. The difference spectra in Figure 4 further support our assignment of the 572 cm^{-1} mode as arising from ν(Fe-O_2) of the oxy cytochrome a_3 species. Figure 4A is the difference spectrum obtained by subtracting the 10 μs Raman spectrum of the enzyme reacted with $^{18}O_2$ from that of the enzyme reacted with $^{16}O_2$. The 572 cm^{-1} peak/548 cm^{-1}

trough pattern is that expected for a mode that shifts 24 cm^{-1} to lower frequency when the heavier O_2 isotope is used. Figure 4B is the difference spectrum obtained by subtracting the 10 μs, high-power spectrum of the enzyme reacted with $^{16}O_2$ from that of the enzyme at 10 μs in the $^{16}O_2$ reaction recorded with lower power. The 572 cm^{-1} peak observed in the spectrum indicates that this mode arises from the photolabile oxy species.

DISCUSSION

Indirect evidence from several laboratories has suggested that the initial intermediate in the reaction of mixed valence cytochrome oxidase with dioxygen is the cytochrome a_3^{2+} - O_2 adduct. Chance and coworkers(9), in their triple trapping experiments, noted the appearance of a 592 nm absorbing species, which they designated as Compound A_1 and formulated as oxycytochrome a_3^{2+}. Hill and Greenwood(7,8) used time-resolved, flow-flash techniques at room temperature to detect a 592 nm chromophore at early times in the oxidation of the mixed valence enzyme. They concurred with the assignment of this species as the dioxygen adduct, although they were unsuccessful in observing a similar chromophore in the reaction of the fully reduced enzyme with O_2. Babcock and Chang(33) showed that the assignment of the 592 nm absorber as an oxygen adduct of ferrous cytochrome a_3^{2+} was consistent with the optical properties of their model imidazole-heme a^{2+} - O_2

complex. The 592 nm absorption maximum, which is the same as that of the CO complex of cytochrome a_3^{2+}, is in agreement with the π-acid properties of dioxygen as a ligand. Babcock, Woodruff and their coworkers(19) used resonance Raman in a time-resolved approach similar to that in the present work to monitor the reaction of the mixed valence enzyme with O_2. They noted that their results indicated the early occurrence of an oxy adduct of cytochrome a_3^{2+}.

By extending the accessible Raman frequency range to low frequencies, we have now been successful in detecting the a_3^{2+} - O_2 adduct by monitoring its ν(Fe-O) motion directly. This measurement complements our recent detection of the analogous vibration at early times in the reaction of the fully reduced enzyme with O_2(23).

An essential aspect of the experiments that have been carried out to monitor the oxidation of cytochrome oxidase by dioxygen is the uniform reliance on photodissociation of CO from its a_3^{2+} binding site as a means by which to initiate the reaction. The reversed electron flow approach developed by Wikstrom(34,35) is a notable exception to this generalization. With the CO photolysis method concerns necessarily arise as to the state of the leaving CO and whether it alters the normal reactivity of the enzyme with O_2. Alben and coworkers(36) showed that CO migrates to the Cu_B^{1+} site in the enzyme following low temperature photolysis of the a_3^{2+}·CO species and Chan(11,12) and his

group suggested that dissociation of the $Cu_B^{1+}\cdot CO$ complex may rate limit subsequent binding and electron transfer events, at least at low temperatures.

Recently, time-resolved Raman(37) and IR(38) spectroscopies have been used to explore the dynamics of CO transient binding and recombination in the a_3^{2+}/Cu_B^{1+} site in detail. Findsen et al.(37) showed that a_3^{2+} relaxes on the μs time scale following photodissociation and that subsequent CO rebinding to the heme iron occurred in ~10 ms. The latter observation is in agreement with earlier optical data(4). Woodruff and coworkers(38) are in the process of an extensive characterization of the CO reaction. Their room temperature results show that, following $a_3^{2+}\cdot CO$ photolysis, the CO migrates to the Cu_B^{1+} site and that essentially complete formation of the $Cu_B^{1+}\cdot CO$ complex occurs in less than 200 ns. By monitoring the $Cu_B^{1+}\cdot CO$ carbonyl stretching vibration directly they have determined that CO dissociates from Cu_B^{1+} in the 1-2 μs range. Rebinding of CO to the a_3^{2+} site proceeds through a pre-equilibrium of the ligand with the Cu_B site; the rate and equilibrium constants involved have been used to estimate that the maximal occupancy of Cu_B^{1+} by CO during the rebinding to a_3^{2+} is ~13%.

These data, in conjunction with those presented here and in our earlier work, suggest minimal perturbation of the cytochrome oxidase/dioxygen reaction by the leaving CO. The 1-2 μs $Cu_B^{1+}\cdot CO$ dissociation rate constant may retard

the binding of O_2 at the a_3^{2+} site somewhat. This is consistent with the 2 μs, low power spectrum in Figure 3, which shows no indication of O_2 binding, and with the work of Hill et al.(8), who noted the occurrence of a spectroscopically silent step after the photolysis of CO and before the formation of the initial reaction intermediate. Nonetheless, the second order rate constant for the interaction with O_2 is on the order of 1 x 10^8 M^{-1} s^{-1}, close to that which would be expected for a diffusion controlled reaction. Once the CO has dissociated from Cu_B^{1+} it appears to equilibrate with bulk solution(38). The subsequent low occupancy of $Cu_B^{1+}\cdot CO$ noted above supports the notion that non-oxygenic events at Cu_B^{1+} will influence the reaction course in only a minor way. Thus the valid concerns of Chan and coworkers(11,12) as to artificial rate limitations imposed by events at Cu_B^{1+} in the formation of, for example, a peroxy intermediate, do not appear to be in force, at least at room temperature.

In our earlier time-resolved work on the mixed valence cytochrome oxidase/O_2 reaction(19), we proposed that the initial intermediate was an oxyhemoglobin-like complex of O_2 with cytochrome a_3^{2+}. The 10 μs, low power spectra in Figures 2 and 3 confirm this hypothesis. In the high frequency region ν_4 shifts from 1355 cm^{-1} in the 2 μs spectrum to 1371 cm^{-1} in the oxy complex, as expected for a π-acid ligand such as O_2. In the 1500-1680 cm^{-1} region overlap with cytochrome a^{3+} modes, which also has an

absorption maximum at 427 nm, congests the spectrum somewhat. Nonetheless, it is clear that the oxy species shows decreased 1570 and 1609 cm^{-1} scattering and increased intensity at 1589 and 1644 cm^{-1}. The former two modes arise from ν_2 and ν_{10} of five-coordinate, high-spin deoxy cyt a_3^{2+}; the shifts in these modes upon oxy complex formation are consistent with the assignment of the cyt a_3/O_2 adduct as a six coordinate, low-spin species. The vinyl mode at 1625 cm^{-1}(17) appears to be relatively insensitive to cyt a_3 ligation but the a_3 formyl upshifts from 1666 cm^{-1} in the 2 μs spectrum to ~1674 cm^{-1} in the oxy complex. The residual 1666 cm^{-1} scattering, as well as that at 1570 cm^{-1}, in the 10 μs, low energy spectrum arises from either incompletely reacted a_3^{2+} or from a small fraction of oxy a_3 complexes that have been photolyzed even by the low energy pulses.

The low frequency spectra in Figures 3 and 4 provide direct detection of the oxy species by way of its iron-oxygen stretching vibration. This mode is located at 572 cm^{-1} in the $^{16}O_2$ spectrum and downshifts to 548 cm^{-1} when the experiment is repeated in $^{18}O_2$. As we observed in the high frequency spectra in Figure 2 and in our earlier work(19), the oxy species is photolabile. The frequency of the iron-oxygen vibration, the magnitude of the isotope shift and the photodissociability of the complex are all consistent with the assignment of this species as the cytochrome a_3^{2+} - O_2 adduct.

Table I summarizes $\nu(Fe^{2+} - O_2)$ frequencies for several heme proteins and model compounds. The 572 cm^{-1} frequency for the mixed valence adduct is essentially identical to the 571 cm^{-1} frequency we measured for this mode during the fully reduced cytochrome oxidase/O_2 reaction(23). Hence, it appears that the $a_3{}^{2+}/O_2$ interaction in the complex is indifferent to the redox state of cytochrome a and Cu_A. This conclusion is consistent with recent work by Caughey and coworkers on carbon monoxy derivatives(43). They reported that, over the range of one to four electron reduction of cytochrome oxidase, the half bandwidth of the C≡O stretching vibration remained essentially constant at ~4 cm^{-1} and that the frequency of this mode shifted only by 2 cm^{-1}. They concluded that the ligand environment of cytochrome a_3 is essentially unaffected by changes in the oxidation states of the other redox centers in the enzyme. Further inspection of Table I shows that ν(Fe-O) in the oxy-cytochrome $a_3{}^{2+}$ species is very similar to that observed for the oxy complexes of the O_2 transport proteins. It is also very close to the $\nu(Fe-O_2)$ frequency we have measured recently in an imidazole-heme $a^{2+} - O_2$ model compound(45). The latter observation, in particular, indicates little perturbation of the bound ligand by cytochrome $a_3{}^{2+}$ pocket effects.[1] Here the situation contrasts somewhat with what has been observed for the CO adduct, as Rousseau and coworkers(44) noted a ν(Fe-CO) in carbon monoxy cytochrome

Table 4.1

Vibrational frequencies for dioxygen bound complexes[a]

	ν(Fe-O)	ref.
Cytochrome oxidase (a^{3+} $a_3{}^{2+}$)	572	This work
Cytochrome oxidase (a^{2+} $a_3{}^{2+}$)	571	(23)
Hb	567	(39)
Mb	570	(40)
HRP III	562	(40)
Im (heme a) Fe^{2+} - O_2	576	(45)
(TMP) Fe - O - O - Fe (TMP)	574	(41)
(Pip) (TPP) Fe^{2+} - O_2	575	(42)
(TPP) Fe^{2+} - O_2	509	(42)

[a]Abbreviations: a^{3+} $a_3{}^{2+}$, mixed valence cytochrome oxidase; a^{2+} $a_3{}^{2+}$ fully reduced cytochrome oxidase; Hb, hemoglobin, Mb, myoglobin; HRP, horseradish peroxidase; Im, imidazole; Pip, piperazine; Fe(TMP), tetramesitylporphyrinatoiron; TPP, meso-tetraphenylporphyrin.

oxidase that was substantially higher than that observed for the CO complexes of other heme proteins.

A clear difference between the mixed valence and fully reduced oxy cytochrome a_3 species, however, is their lifetimes. Hill et al.(6,7) reported that the oxy intermediate in the fully reduced enzyme was undetectable owing to its short lifetime. We interpreted our earlier Raman data(18) to indicate that the oxy species was detectable and that it decayed with a halftime consistent with a rate constant of ~ 2×10^4 s^{-1} at 25°C. Orii's optical data(16) and our recent Raman data on ν(Fe-O) in the a_3^{2+}/O_2 adduct confirm the detectability of this species; there is some disagreement, however, as to its decay rate constant and this merits further study. It is clear, however, that the mixed valence oxy species reacts to form subsequent species at a substantially slower rate than the fully reduced enzyme. Hill et al.(8) and Orii(16) detected this species optically and we estimated a decay rate constant of ~ 3.5×10^3 s^{-1} in our earlier Raman work(19), in reasonable agreement with the value of 6×10^3 s^{-1} reported by Hill et al.(8). The data in Figure 1 are consistent with these rate constants as photostable intermediates are formed in the 100-500 μs time regime. In the 500 μs spectrum the position of ν_4 at 1371 cm^{-1} and of the formyl at 1674 cm^{-1} indicates that cytochrome a_3 is oxidized. Moreover, its ν_2 vibration has shifted underneath the ν_2 vibration of low-spin cytochrome a^{3+} at

1589 cm^{-1}. This indicates the formation of a low-spin or intermediate-spin(30) cytochrome a_3^{3+} complex at 500 μs in agreement with the optical data reported by Greenwood et al.(8). The relationship of this species to trapped intermediates in the mixed valence/O_2 reaction, to species that occur at longer times, and to forms of the enzyme that occur when the oxidized enzyme reacts with H_2O_2 is under investigation.

REFERENCES

1. Wikstrom, M., Krab, K. and Saraste, M. (1981), "Cytochrome Oxidase, A Synthesis", Acad. Press, New York.
2. Caughey, W.S., Smythe, G.A., O'Keeffe, D.H., Maskasky, J. and Smith, M.L. (1975) J. Biol. Chem. **250**, 7602-7622.
3. Einasdottir, O. and Caughey, W.S. (1984) Biochem. Biophys. Res. Commun. **124**, 836-842.
4. Gibson, Q. and Greenwood C. (1963) Biochem. J. **86**, 541-554.
5. Greenwood, C. and Gibson, Q. (1967) J. Biol. Chem. **242**, 1782-1787.
6. Hill, B. and Greenwood, C. (1984) Biochem. J. **218**, 913-921.
7. Hill, B., Greenwood C. and Nichols, P. (1986) Biochim. Biophys. Acta **853**, 91-113.
8. Hill, B.C. and Greenwood, C. (1983) Biochem. J. **215**, 659-667.
9. Chance, B., Saronio, C. and Leigh, J.S. (1975) J. Biol. Chem. **250**, 9226-9237.

10. Clore, G.M., Andreasson, L.E., Karlsson, B., Aasa, R. and Malmstrom, B.G. (1980) Biochem. J. **185**, 139-154.

11. Chan, S.I., Witt, S.N. and Blair, D.F. (1988) Chemica Scripta **28A**, 51-56.

12. Blair, D.F., Witt, S.N. and Chan, S.I. (1985) J. Am. Chem. Soc. **107**, 7389-7399.

13. Denis, M. (1981) Biochim. Biophys. Acta, **634**, 30-40.

14. Chance, B., Saronio, C. and Leigh, J.S. (1975) Proc. Natl. Acad. Sci. U.S.A. **72**, 1635-1640.

15. Orii, Y. (1984) J. Biol. Chem. **259**, 7187-7190.

16. Orii, Y. (1988) Annals of the New York Academy of Science **550**, 105-117.

17. Babcock, G.T. (1988) "Biological Applications of Raman Scattering" (Spiro, T.G., ed.), Vol. 3, 295-346.

18. Babcock, G.T., Jean, J.M., Johnston, L.N., Palmer, G. and Woodruff, W.H. (1984) J. Am. Chem. Soc. **106**, 8305-8306.

19. Babcock, G.T., Jean, J.M., Johnston, L.N., Woodruff, W.H. and Palmer, G. (1985) J. Inorg. Biochem. **23**, 243-251.

20. Ogura, T., Yoshikawa, S. and Kitagawa, T. (1985) Biochim. Biophys. Acta **832**, 220-223.

21. Ogura, T., Yoshikawa, S. and Kitagawa, T. (1989) Biochemistry **28**, 8022-8027.

22. Han, S., Ching, Y.-C., and Rousseau, D.L. (1989) J. Biol. Chem. **264**, 6604-6607.

23. Varotsis, C., Woodruff, W.H. and Babcock, G.T. (1989)

J. Am. Chem. Soc. **111**, 6439-6440; (1990) **112**, 1297.

24. Hartzell, R. and Beinert, H. (1974) Biochim. Biophys. Acta. **368**, 318-338.

25. Vanneste, W.H. (1966) Biochemistry **5**, 838-847.

26. Varotsis, C., Oertling, W.A. and Babcock, G.T. (1990) App. Spectroscopy, in press.

27. Babcock, G.T., Callahan, P.M., Ondrias, M.R. and Salmeen, I. (1981) Biochemistry **20**, 959-966.

28. Woodruff, W.H., Dallinger, R.F., Antalis, T.M. and Palmer, G. (1981) Biochemistry **20**, 1332-1338.

29. Argade, P.V., Ching, Y.-C. and Rousseau, D.L. (1986) Biophys. J. **50**, 613-620.

30. Carter, K.R., Antalis, T.M., Palmer, G.M., Ferris, N.S. and Woodruff, W.H. (1981) Proc. Natl. Acad. Sci. U.S.A. **78**, 1652-1655.

31. Ching, Y.-C., Argade, P. and Rousseau, D. (1985) Biochemistry **24**, 4938-4946.

32. Rousseau, D.L., Singh, S., Ching, Y.-C. and Sassaroli, M. (1988) J. Biol. Chem. **263**, 5681-5685.

33. Babcock, G.T. and Chang, C.K. (1979) FEBS Lett. **97**, 358-362.

34. Wikstrom, M. (1981) Proc. Nat. Acad. Sci. U.S.A. **78**, 4051-4053.

35. Wikstrom, M. (1989) Nature **338**, 776-778.

36. Alben, J.O., Moh, P.P., Fiamingo, F.G. and Altschuld, R.A. (1981) Proc. Natl. Acad. Sci. U.S.A. **78**, 234-237.

37. Findsen, E.W., Centeno, J., Babcock, G.T. and Ondrias,

M.R. (1987) J. Am. Chem. Soc. **109**, 5367-5372.

38. Dyer, R.B., Einarsdottir, O., Killough, P.M., Lopez-Garriga, J.J. and Woodruff, W.H. (1989) J. Am. Chem. Soc. **111**, 7657-7659.

39. Brunner, H. (1974) Naturwissenschaften **61**, 129-130.

40. Van Wart, H. and Zimmer, J. (1985) J. Biol. Chem. **250**, 8372-8377.

41. Paeng, I.R., Shiwaku, H. and Nakamoto, K. (1988) J. Am. Chem. Soc. **110**, 1995-1997.

42. Nakamoto, K., Paeng, I.R., Kuroi, T., Iosbe, T. and Oshio, H. (1988) J. Mol. Struct. **189**, 293-300.

43. Einarsdottir, Olof, Choc, M.G., Weldon, S. and Caughey, W. (1988) J. Biol. Chem. **263**, 13641-13654.

44. Argade, P.V., Ching, Y.-C. and Rousseau, D.L. (1984) Science, **225**, 329-331.

45. Oertling, W.A., Kean, R.T., Wever, R., and Babcock, G.T. (1990) Inorg. Chem., in press.

CHAPTER 5

LATE APPEARANCE OF THE ν (Fe^{IV}=O) VIBRATION FROM A FERRYL-OXO INTERMEDIATE IN THE CYTOCHROME OXIDASE/DIOXYGEN REACTION*

SUMMARY

Time-resolved resonance Raman spectra have been recorded during the reaction of fully-reduced ($a^{2+}a_3{}^{2+}$) cytochrome oxidase with dioxygen at room temperature. In the spectrum recorded at 800 μs subsequent to carbon-monoxide photolysis a mode is observed at 790 cm^{-1} that shifts to 755 cm^{-1} when the experiment is repeated with $^{18}O_2$. The frequency of this vibration and the magnitude of the $^{18}O_2$ isotopic frequency shift lead us to assign the 790 cm^{-1} mode to the Fe^{IV}=O stretching vibration of a ferryl-oxo cytochrome a_3 intermediate that occurs in the reaction of fully-reduced cytochrome oxidase with dioxygen. The appearance and vibrational frequency of this mode were not affected when D_2O was used as a solvent. This result suggests that the ferryl-oxo intermediate is not hydrogen-

---

*Varotsis, C. and Babcock, G. T. (1990), submitted.

bonded. We have also recorded Raman spectra in the high-frequency (1000-1700 cm^{-1}) region during the oxidase/O_2 reaction that show that the oxidation of cytochrome a^{2+} is biphasic. The faster phase is complete within 100 μs and is followed by a plateau region in which no further oxidation of cytochrome a occurs. The plateau persists to ~500 μs and is followed by the second phase of oxidation. These results on the kinetics of the redox activity of cytochrome a are consistent with the branched pathway discussed by Hill, Greenwood, and Nichols (Biochim. Biophys. Acta 853, 91-113 (1986)) for the oxidation of reduced cytochrome oxidase by O_2 at room temperature. Within the context of this scheme, the ferryl-oxo intermediate we have observed arises as the fourth and final electron enters the dioxygen reduction site.

INTRODUCTION

In the mitochondrial electron transport chain of eucaryotic organisms, cytochrome oxidase functions as the oxygen-activating enzyme. The overall reaction catalyzed by the enzyme is the rapid reduction of dioxygen to water. The free energy released in the electron-transfer reactions that occur during O_2 reduction is conserved as an electrochemical proton gradient across the inner mitochondrial membrane and is used ultimately for adenosine triphosphate synthesis(Wikstrom et al., 1981). Mitochondrial cytochrome c oxidase contains two hemes, cytochrome a and a_3, and two

copper atoms, designated Cu_A and Cu_B. The low potential sites, cytochrome a and Cu_A, function together in the sense that they oxidize cytochrome c and subsequently transfer the reducing equivalents to the high-potential binuclear site, which contains cytochrome a_3 and Cu_B, where oxygen binding and reduction to H_2O take place.

Although the cytochrome oxidase/dioxygen reaction has been extensively studied by various spectroscopic techniques at room and low temperatures(Gibson and Greenwood, 1963; Hill and Greenwood, 1983, 1984; Hill, et al., 1986; Orii, 1984, 1988; Oliveberg et al., 1990; Chance et al., 1975a,b; Clore et al., 1980; Blair et al., 1985; Chan et al., 1988), the reaction mechanism is not yet fully understood. For example, the precise chemical identity of various intermediates and the pathway(s) by which electrons are transferred to the binuclear site are important mechanistic questions for which further information is required. The reaction is rapid under physiological conditions ($t_{1/2}$ = 1 ms)(Gibson and Greenwood, 1963; Greenwood and Gibson, 1967). Nonetheless, the room-temperature flow/flash technique developed by Gibson and Greenwood(1963), has provided a way to resolve the reaction kinetically. Hill and Greenwood(1983; 1984), Orii(1984; 1988) and Oliveberg et al.(1990) used this technique to show that partially-reduced intermediates were generated at room temperature. Chance et al.(1975a,b), Clore et al.(1980), Blair et al.(1985), and Chan et al.(1988) studied intermediates involved in dioxygen

reduction at low temperatures and characterized them by using optical and EPR spectroscopies. Wikstrom(1981, 1989) was able to reverse electron flow through the enzyme to trap what was postulated to be a peroxy intermediate that precedes ferryl-oxo formation in the reaction scheme he proposed.

Wikstrom(1989), Blair et al.(1985), and Chan et al.(1988) have postulated heterolytic cleavage of the O=O bond to form a cytochrome a_3 ferryl-oxo (Fe^{IV}=O) intermediate as electrons from the cytochrome a/Cu_A sites enter the oxygen-bound binuclear site. The formation and decay rates of intermediate species in this process are not well determined at room temperature, although recently Orii(1988) proposed that a ferryl-oxo species occurs at ~100 μs in the oxidase/dioxygen reaction, consistent with the rapid oxidation of a fraction of the a/Cu_A centers that has been inferred from optical measurements(Hill and Greenwood, 1984; Hill et al., 1986). Furthermore, the protonation steps involved, as well as the specific structure of the cytochrome a_3/O_2 adducts, are not yet well defined, although a variety of structures have been postulated(Hill and Greenwood, 1983; 1984; Hill et al. 1986; Chance et al., 1975a,b; Clore et al., 1980; Blair et al., 1983; 1985; Chan et al., 1988; Oliveberg et al., 1990).

Raman spectroscopy is a structure-specific vibrational technique and, relative to optical or EPR spectroscopies, has the potential to provide more detailed information on

the intermediate structures that occur during the oxidation of cytochrome oxidase by O_2. Babcock et al.(1984; 1985), using pulsed excitation, and later Ogura et al.(1985; 1989), with continuous-wave lasers, showed that a time-resolved Raman approach was feasible. Although a photolabile cytochrome a_3^{2+}-O_2 species was postulated as the initial intermediate in O_2 reduction in this work (Babcock et al., 1984), the measurements were confined to the high-frequency region. Recently, Varotsis et al.(1989; 1990a), Han et al.(1990a; 1990b), and Ogura et al.(1990) have confirmed the occurrence of this oxy species by monitoring the $\nu(Fe_{a_3}^{2+}$-$O_2)$ vibration directly in the reaction of both the mixed valence and fully-reduced enzyme with O_2.

In the experiments reported here, we have continued the two-color, pulsed irradiation Raman approach to intermediates that occur at later times in the fully-reduced cytochrome oxidase/dioxygen reaction. The pulsed technique is particularly useful in this application, as the time resolution is determined by the programmable time delay between the short (10 ns) pump and probe laser flashes. This contrasts with a c. w. laser approach in which the time resolution is determined by the residence time of the reacting sample in the beam. The latter approach becomes ambiguous kinetically as this residence time increases. Our results indicate that cytochrome a is oxidized in a biphasic manner. Partial oxidation occurs at early times after mixing ($t<100\ \mu s$), consistent with optical data reported by

several workers (Hill and Greenwood, 1984; Hill et al. 1986; Orii, 1988; Brunori and Gibson, 1983; Oliveberg et al., 1990) and with branched schemes for the overall reaction (Hill and Greenwood, 1984; Hill et al. 1986; Clore et al., 1980; Blair et al., 1983; 1985; Chan et al., 1988). Despite this agreement with the absorption experiments, there is no clear indication of a conventional ferryl-oxo species at this three-electron level of reduction. Instead, we detect $\nu(Fe^{IV}=O)$ at later times in the reaction ($t \approx 800$ μs), as the more slowly-reacting fraction of cytochrome a is oxidized. The frequency of this ferryl-oxo stretching motion, 790 cm^{-1}, is insensitive to H_2O/D_2O exchange, suggesting that it is not hydrogen bonded. Within the context of the branched kinetic schemes that have been developed from the earlier spectroscopic work, the appearance of this ferryl accompanies the arrival of the fourth electron in the oxygen-bound binuclear site.

EXPERIMENTAL PROCEDURES

Cytochrome oxidase was prepared from beef hearts by using a modified Hartzell-Beinert(1974) preparation and was frozen under liquid N_2 until ready for use. The enzyme was solubilized in 50 mM HEPES (4-(2-hydroxyethyl)-1-piperazineethanesultonic acid) at pH 7.4 with 0.5% dodecyl β-D-maltoside. The absorption spectrum of resting cytochrome oxidase shows a maximum at 421 nm, which is characteristic of rapidly-reacting enzyme. The fully-

reduced, carbon-monoxide-bound enzyme was prepared by anaerobic reduction with 4 mM sodium ascorbate and 1 μM cytochrome c under CO and shows a Soret maximum at 430 nm, as expected (Vanneste, 1966). The pD of solutions prepared in D_2O buffer was measured by using a pH meter and assuming pD=pH (observed) +0.4. The experimental techniques used for the measurements of time-resolved Raman spectra have already been reported(Varotsis, et al., 1989; 1990a,b). The probe wavelength (441 nm) was provided by pumping coumarin 440 with the third harmonic output (355 nm) of a quanta-ray DCR 2A pulsed laser.

RESULTS

Figure 1 shows high-frequency resonance Raman spectra of fully-reduced ($a^{2+}a_3{}^{2+}$) cytochrome oxidase at various delay times subsequent to carbon-monoxide photolysis in the presence of O_2. With 427 nm excitation, cytochrome a^{2+} and cytochrome $a_3{}^{2+}$ contribute roughly equally to the resonance Raman spectrum of the fully-reduced enzyme through an 0-1 enhancement mechanism because of their coincident absorption maxima near 443 nm(Babcock et al., 1981; Woodruff et al., 1981; Argade et al., 1986; Babcock, 1988). Excitation at 427 nm also enhances vibrations of cytochrome a^{3+} and those of oxygenated cytochrome a_3, which have absorption maxima in the 427-nm range. In the 10-ns photoproduct spectrum (Figure 1A), the oxidation state marker is at 1355 cm^{-1}, establishing that both cytochromes are in the ferrous state.

Figure 5.1 Time-resolved resonance Raman spectra of fully-reduced cytochrome oxidase at the indicated times. The energy of the 532-nm photolysis pump/pulse was 1.3 mJ, sufficient to photolyze the enzyme-CO complex and initiate the O_2-reduction reaction. The energy of the 427-nm probe beam was 0.8 mJ for spectra A and F and 0.3 mJ for Spectra B-E. The repetition rate for both the pump and probe pulses (10-ns duration) was 10 Hz. The accumulation time was 15 min for Spectra A and F and 50 min for Spectra B-E. The enzyme concentration was 50 μM after mixing, pH 7.4.

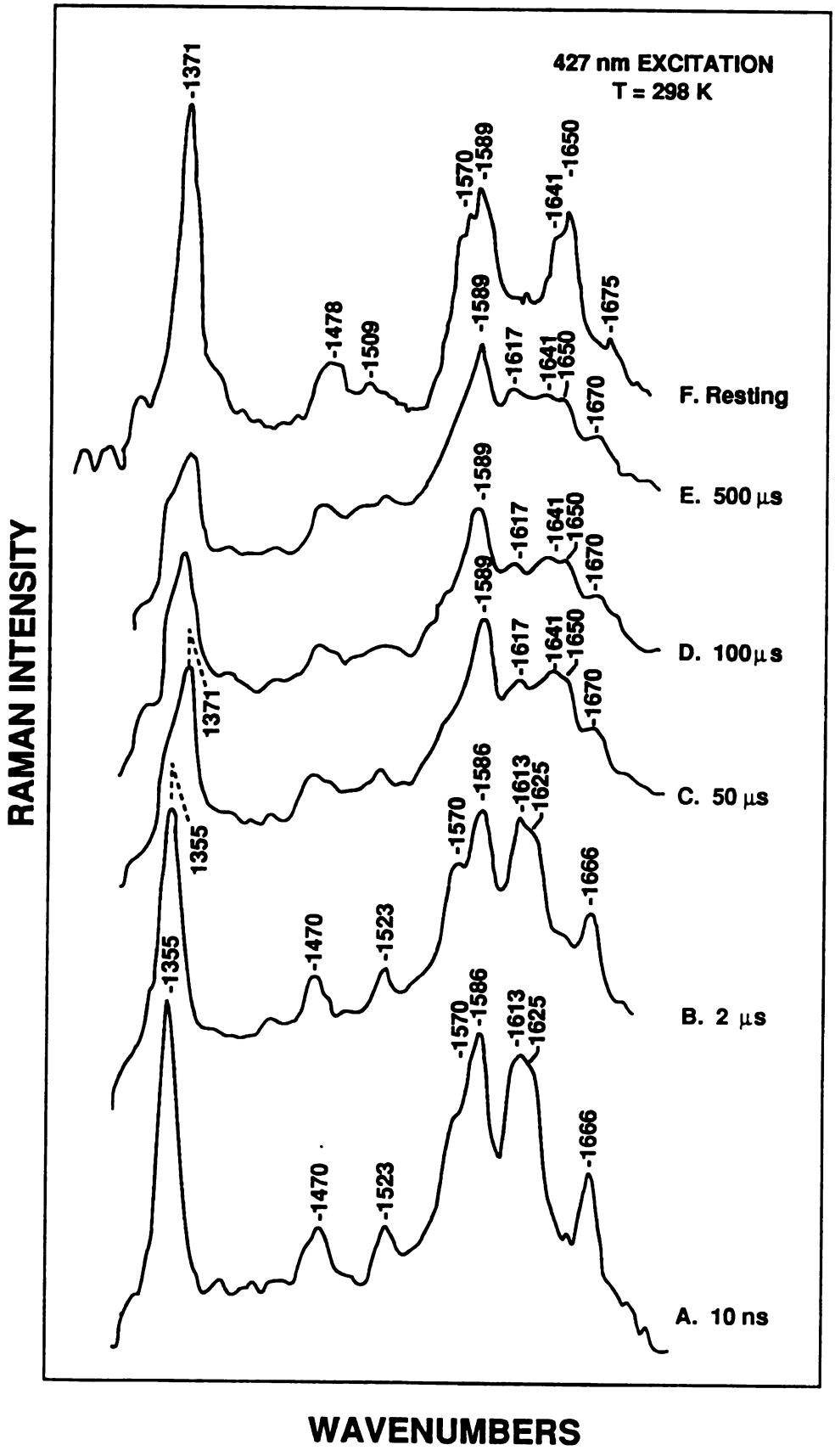
427 nm EXCITATION
T = 298 K
RAMAN INTENSITY
WAVENUMBERS
F. Resting
E. 500 μs
D. 100 μs
C. 50 μs
B. 2 μs
A. 10 ns
1371
1478
1509
1570
1589
1641
1650
1675
1617
1670
1355
1470
1523
1586
1613
1625
1666

The core expansion region shows two vibrations at 1570 cm^{-1} and 1586 cm^{-1}. The 1622 cm^{-1} mode arises from the C=C stretching vibration of cytochromes a^{2+} and $a_3{}^{2+}$. The 1613 cm^{-1} and 1666 cm^{-1} modes have been assigned(Babcock et al., 1981; Babcock, 1988) as the C=O stretching vibration of the formyl group (-CHO) of a^{2+} and $a_3{}^{2+}$, respectively. Spectrum B shows that no significant changes are detected at 2 μs in the reaction, consistent with our earlier results(Varotsis et al., 1989; 1990a).

As the reaction proceeds, oxidation of cytochrome a_3 and a occurs. At 50 μs, the oxidation state marker has shifted to 1371 cm^{-1} and the shoulder at 1358 cm^{-1} is substantially decreased, indicating that an oxygen adduct of cytochrome a_3 is formed in this reaction(Babcock et al., 1984; Varotsis et al., 1989; Han et al., 1990b; Ogura et al., 1990). The cytochrome a_3 core-size band, ν_2, which appears at 1570 cm^{-1} in the 10-ns and 2-μs spectra, shifts to higher frequency in the 50-μs spectrum and overlaps with the ν_2 vibration of cytochrome a^{2+}, which is located at 1589 cm^{-1}. Evidence for six-coordination may be seen by the appearance of the ν_{10} of cytochrome a_3 at 1641 cm^{-1}. The decrease in intensity of the 1613 cm^{-1} mode and the concomitant increase in scattering at 1650 cm^{-1} indicate that partial oxidation of cytochrome a has occurred at 50 μs. A similar conclusion concerning partial oxidation of cytochrome a was reached by Hill and Greenwood (1984), Hill et al. (1986) and Orii(1988) in their optical absorption

measurements. The formyl vibration of cytochrome a_3, which is located at 1666 cm^{-1} in the photoproduct spectrum, has lost intensity and shifted to 1670 cm^{-1} as oxy cytochrome a_3 and subsequent oxidation products are formed. Following this burst of redox activity in the first 100 μs, the Raman spectra show little change in the 100-500 μs time range. In particular, oxidation of cytochrome a remains partial, as indicated by the 1358 cm^{-1} shoulder in the ν_4 region in the 500-μs spectrum. The second phase of a oxidation occurs in the 500 μs– 5 ms time range to produce the oxidized enzyme(Babcock et al., 1984).

The kinetic behavior of the enzyme, as detected by Raman spectroscopy, is similar to behavior that has been observed in optical experiments. Hill and Greenwood(1984) and Hill et al. (1986) observed biphasic oxidation of cytochrome a with halftimes of 35 μs and 860 μs. The amplitudes of the two phases were 0.4 and 0.6, respectively. These authors also noted biphasic Cu_A oxidation with similar rate constants but with relative amplitudes of 0.6 and 0.4, respectively. Phenomenologically similar data on heme redox activity were reported by both Orii(1988) and by Brunori and Gibson(1983), i.e., a rapid phase of cytochrome oxidation, followed by a plateau period extending to about 500 μs, and subsequent completion of heme oxidation. To explore further the oxidation of cytochrome a, we have obtained Raman spectra with 441-nm excitation (Figure 2), which should enhance vibrational modes of cytochrome a^{2+} extensively in

Figure 5.2 Time-resolved resonance Raman spectra of fully-reduced cytochrome oxidase at the indicated times. The energy of the 532-nm photolysis pump/pulse was 1.3 mJ. The energy of the 441-nm probe beam was 0.8 mJ for Spectrum A and 0.3 for Spectrum B. The repetition rate for both the pump and probe pulses was 10 Hz. The accumulation time was 15 min for Spectrum A and 65 min for Spectrum B. The enzyme concentration was 50 μM after mixing, pH 7.4.

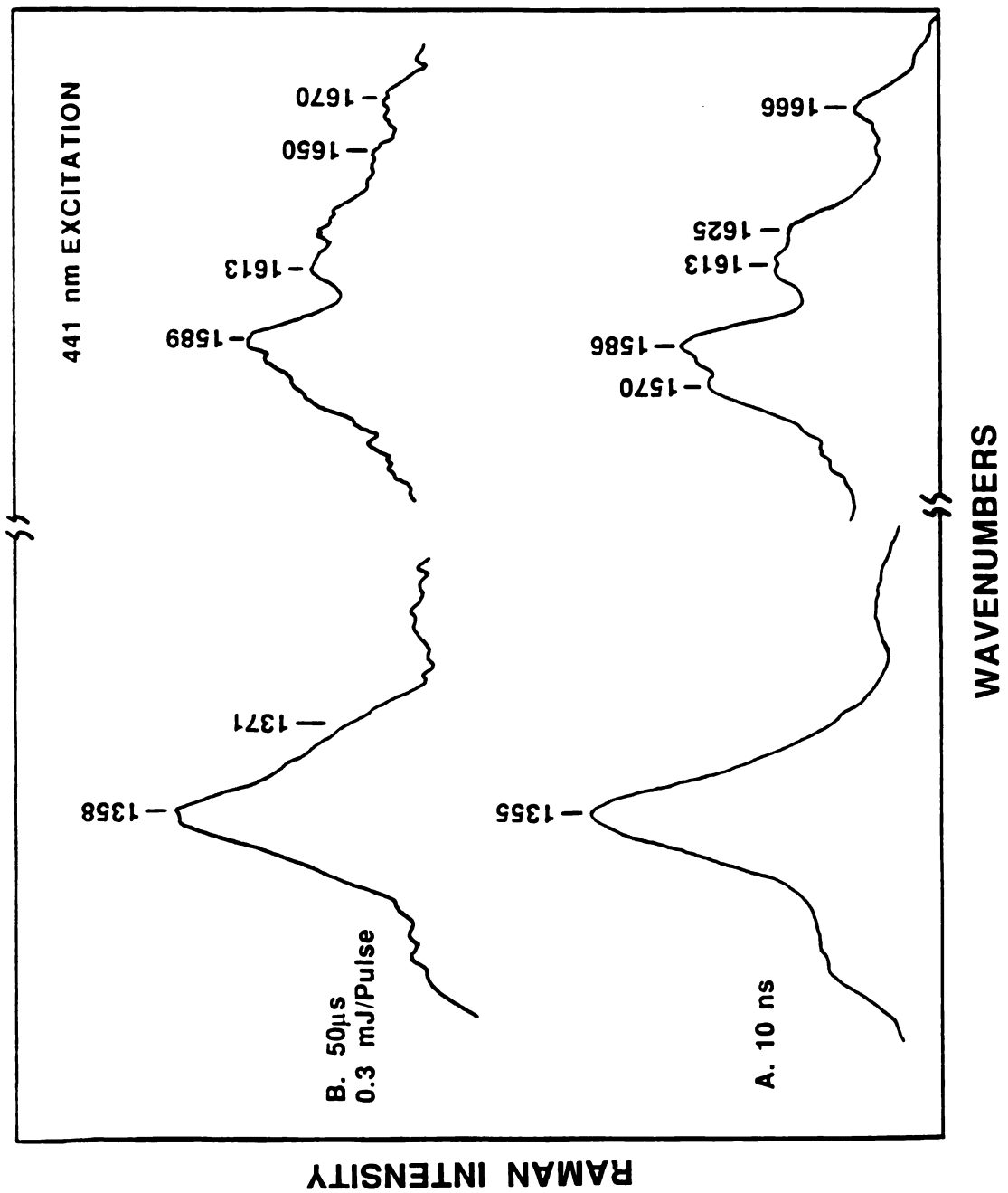
441 nm EXCITATION
1670
1650
1613
1589
1371
1358
B. 50μs
0.3 mJ/Pulse
1666
1625
1613
1586
1570
1355
A. 10 ns
WAVENUMBERS
RAMAN INTENSITY

the reaction-time course, as oxygen-bound cytochrome a_3 intermediates are expected to have substantially blue-shifted absorption spectra. The 50-μs spectrum indicates that oxidation of cytochrome a, as judged by the decreased scattered intensity of modes characteristic of cytochrome a^{2+} and the increased scattered intensity of the cytochrome a^{3+} formyl mode at 1650 cm^{-1}, has occurred and further supports the data obtained with 427-nm excitation.

The high-frequency data indicate partial oxidation of cytochrome a at 100 μs. Coupled with the complementary partial oxidation of Cu_A in the same time range that has been observed optically, these results indicate the formation of a three-electron-reduced $a_3/Cu_B/O_2$ site in a large fraction of the reacting enzyme. A number of chemically-interesting species have been suggested for the three-electron-reduced intermediate including ferryl-oxo and ferrous-hydroperoxide structures(Wikstrom, 1981; Wikstrom et al., 1981; Blair et al., 1983; 1985; Chan et al., 1988); and, indeed, Orii(1988) interpretted his optical data to indicate cytochrome a_3 ferryl-oxo formation at 100 μs in the reaction. In extensive investigations of the intermediate frequency region at 100, 300 and 500 μs in the reaction, however, we have seen no clear and reproducible indication of conventional ferryl species, which is expected in the 740-850 cm^{-1} range (see Table I, below). Our failure, thus far, to observe such a mode unambiguously is certainly not an indication that a ferryl species does not occur at the

three-electron level of reduction, and we are continuing our studies of this time regime.

By extending the pump-probe delay to times longer than 500 μs, we have continued our study of the reaction time course by recording Raman spectra in the 550-850 cm^{-1}-frequency range during the slower phase of cytochrome a oxidation. These spectra are shown in Figure 3. Spectrum 3A is that of the photodissociation product of the fully-reduced carbonmonoxy enzyme (t_d=10 ns). The ν_7 and ν_{16} modes located at 685 cm^{-1} and 749 cm^{-1}, have contributions from both cytochrome a_3^{2+} and cytochrome a^{2+}(Argade et al., 1986). Spectrum B (t_d=500 μs) and Spectrum C (t_d=800 μs) are similar to the 10-ns spectrum with the exception that a new mode appears at 790 cm^{-1} in the 800 μs spectrum. Figure 3D shows that the 790 cm^{-1} mode in the $^{16}O_2$ spectrum disappears when the experiment is repeated with $^{18}O_2$. By subtracting the $^{18}O_2$ spectrum (Figure 3D) from that obtained with $^{16}O_2$ (Figure 3C), we obtain Figure 3F. This difference spectrum shows that the 790 cm^{-1} mode in the $^{16}O_2$ spectrum shifts down by 35 cm^{-1} to 755 cm^{-1} in the presence of $^{18}O_2$; in the absolute spectrum of the heavier oxygen isotope, the 755 cm^{-1} mode is obscured by the ν_{16} macrocycle mode at 749 cm^{-1}. These spectra demonstrate that an oxygen-isotope sensitive mode occurs at 790 cm^{-1} at 800 μs in the reaction between O_2 and reduced cytochrome oxidase. The frequency of this mode and the 35 cm^{-1} isotope shift, which is in good agreement with that predicted by a two-body FeO harmonic

Figure 5.3 Time-resolved resonance Raman spectra of fully-reduced cytochrome oxidase following initiation of the reaction with oxygen at room temperature. The energy of the 532-nm photolysis pump/pulse was 1.3 mJ. The energy of the 427-nm probe beam was 0.8 mJ for all spectra. The repetition rate for both the pump and probe pulses was 10 Hz. The accumulation time was 15 min for Spectrum A and 20 min for Spectra B-E. The enzyme concentration was 50 μM after mixing, pH 7.4.

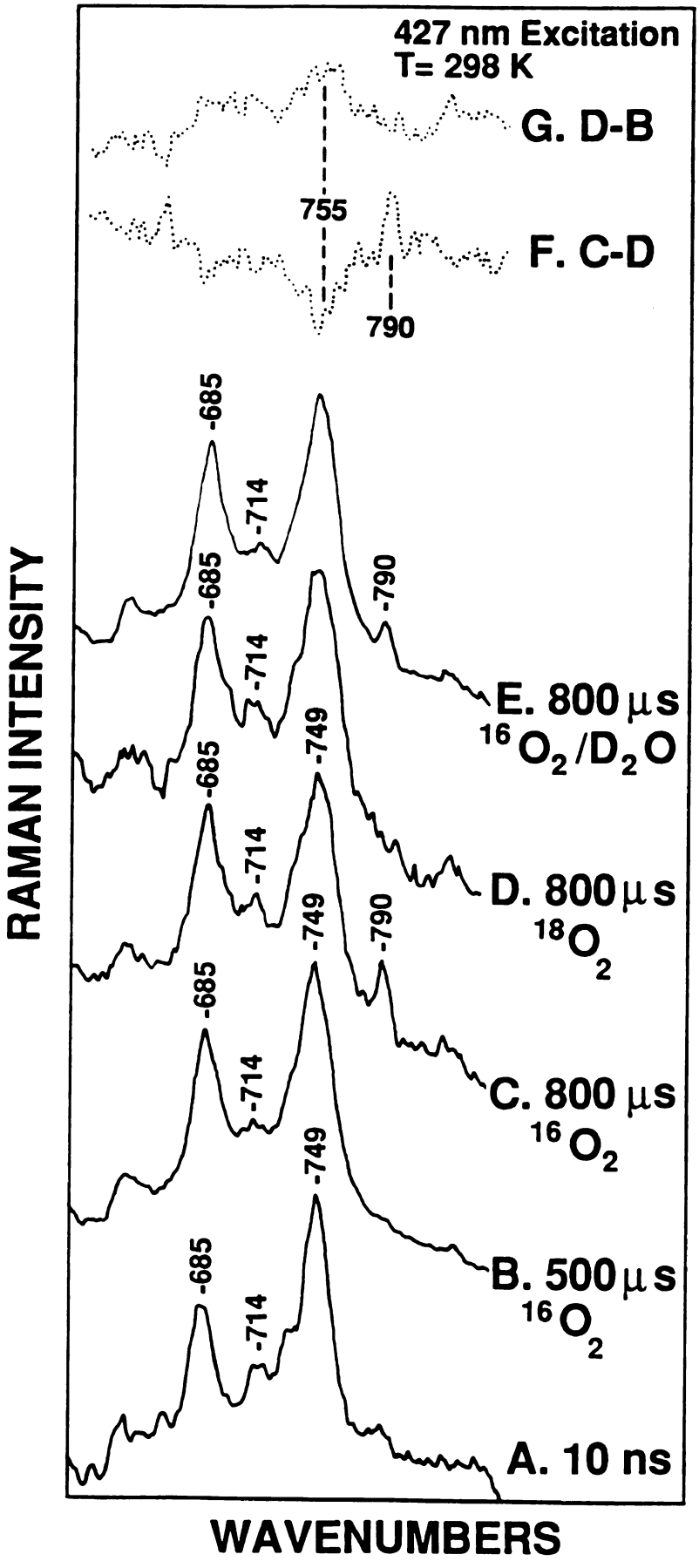
427 nm Excitation
T= 298 K
G. D-B
755
F. C-D
790
-685
-714
-790
E. 800 μs
16O2/D2O
-685
-714
-749
D. 800 μs
18O2
-685
-714
-749
-790
C. 800 μs
16O2
-685
-714
-749
B. 500 μs
16O2
-685
-714
-749
A. 10 ns
RAMAN INTENSITY
WAVENUMBERS

oscillator approximation, indicates that this vibration arises from a ferryl-oxo (Fe^{IV}=O) cytochrome a_3 species (see below). Figure 3E shows the 800-μs spectrum of the cytochrome oxidase/$^{16}O_2$ solution prepared in D_2O. Comparison of Figure 3C with Figure 3E shows that similar results for $\nu(Fe^{IV}=O)$ are obtained in H_2O and D_2O buffers. This implies that there is no hydrogen bonding of the ferryl-oxo intermediate at pH 7.4.

DISCUSSION

The oxidation of cytochrome oxidase has been studied extensively by both optical and EPR spectroscopies and a variety of schemes has been proposed for the intramolecular transfer of electrons to the dioxygen-reducing site. The original formulation of Gibson and Greenwood(1963) involved sequential transfer to the oxygen-bound binuclear site, with Cu_A and then cytochrome a undergoing oxidation. Hill and Greenwood(1984) later attempted to reconcile this scheme with the extinction coefficients that have been established for a and a_3 and found that in order to do this it was necessary to introduce a branch in the room-temperature reaction pathway such that oxidation of both cytochrome a and Cu_A occurred biphasically with a fast phase of $\leqslant$ 100 μs and a slower phase in the 800-μs time range. Clore et al.(1980) and Chan and co-workers(Blair et al., 1985; Chan et al., 1988) were led to a similar branched pathway in order to interpret low-temperature optical and EPR data. In

terms of the dioxygen-reducing site, these schemes suggest that the third electron in O_2 reduction is transferred in a branched fashion from either a or Cu_A and that the fourth electron is then transferred from the remaining, unoxidized center.

In room-temperature, time-resolved optical work, this branched pathway is manifested by a burst of cytochrome oxidation at t < 100 μs followed by a plateau, and final cytochrome oxidation in the slower phase. Thus the three-electron intermediate would form in times less than 100 μs and be accompanied by partial cytochrome a oxidation. The fourth electron would be transferred in the 800-μs range. Although the details of the interpretations vary, phenomenologically similar observations as to the time course of cytochrome oxidation have been made at room temperature by Orii(1988), by Malmstrom and co-workers(Oliveberg et al., 1990), and by Brunori and Gibson(1983).

The Raman data we report in Figures 1 and 2 are consistent with this branched mechanism. At early times in the reaction (t < 100 μs), we observe partial oxidation of cytochrome a with both 427 nm and 441 nm excitation, along with oxygenation and oxidation of cytochrome a_3. Following this rapid phase, which we associate with the formation of a three-electron reduced-dioxygen site, the system undergoes little detectable change to 500 μs. Entry of the fourth electron is associated with the slow phase that extends from

500 μs to about 5 ms.

Within the context of this scheme, which is consistent with the bulk of the optical, EPR, and resonance Raman data, the three electron reduced intermediate would persist from ~ 100 μs to ~ 500 μs. Wikstrom(1981, 1989), by reversing the dioxygen reaction in mitochondria, noted the appearance of a 580-nm absorbing species which he proposed as the one-electron oxidation product of the a_3^{3+}/Cu_B^{2+} couple. In addition, he proposed ferryl-oxo structures for both the three- and four-electron reduced intermediates. Chan and co-workers(Blair et al., 1985; Chan et al., 1988) detected a 580/537-nm species in the three electron reduced enzyme/O_2 reaction and suggested the formation of two three-electron, reduced intermediates. They proposed that the first species, which is EPR-detectable, is a hydroperoxide-bridged Cu_B^{2+}/a_3^{2+} adduct and that the second intermediate is a Fe^{IV}=O/Cu_B^{2+} species formed by cleavage of the O-O bond in the hydroperoxide adduct with uptake of a proton. Clore et al.(1980) have also postulated the formation of a ferryl-oxo adduct. In addition, the 100-μs difference spectrum reported by Orii(1988) resembles the optical spectra of Chan et al.(1988), Clore et al.(1980), and Wikstrom(1981, 1989). He noted that his results indicated the early occurrence of a three-electron reduced intermediate and proposed an oxo-ferryl cytochrome a_3 structure for this adduct. As already discussed, we see no clear evidence for a conventional ferryl-oxo species in our 550-850 cm^{-1} data at 100, 300, and

500 μs in the reaction. The three electron level of reduction is likely to involve substantial nuclear rearrangement in the dioxygen site (Blair et al., 1985), however, and thus it is quite possible that the bound dioxygen species undergoes valence change, bond rearangement, and protonation reactions before the arrival of the fourth electron. If the rates for these reactions are comparable, then at any given time, the site will exist in a variety of different configurations. Such a situation would render Raman detection, already difficult for relatively-homogeneous populations, problematic.

It is clear, however, from our data that a ferryl-oxo intermediate, detected by its iron-oxygen stretching vibration, does occur during dioxygen reduction. The data of Figure 3 indicate that this species is formed at 800 μs in the reaction sequence, which is substantially later than three electron reduced intermediates are expected. The iron-oxygen stretching mode is located at 790 cm^{-1} in the 800-μs spectrum and downshifts to 755 cm^{-1} when the experiment is repeated with $^{18}O_2$. The frequency of the iron-oxygen vibration and the magnitude of the isotope shift are both consistent with the assignment of this species as the ferryl-oxo cytochrome a_3 adduct. Moreover, the ferryl-oxo intermediate is absent in the 500-μs spectrum but present at ~800 μs, which is consistent with the half times reported by Hill and Greenwood(1984); Hill et al.(1986), and Oliveberg et al.(1990) for the formation of a four-electron

reduced intermediate. The most reasonable assignment of the 790 cm^{-1} mode is that it arises from a $Cu_A^{2+}a^{3+}a_3^{4+}=O/Cu_B^{1+}$ complex. Such a structure has been proposed for the four-electron reduced complex by Wikstrom(1981).

Table I summarizes $\nu(Fe^{IV}=O)$ frequencies for several heme proteins and model compounds. The 790 cm^{-1} frequency for the ferryl-oxo cytochrome a_3 adduct is similar to the 787 cm^{-1} frequency reported by Terner and co-workers(Sitter et al.(1985b)) as well as by Hashimoto et al.(1984) and Oertling et al.(1988) for $\nu(Fe^{IV}=O)$ of HRP compound II but slightly lower than that observed by Sitter et al.(1985a) for Mb=O ($\nu(Fe^{IV}=O)$ = 797 cm^{-1}) and ~30 cm^{-1} lower than that observed by Kean et al.(1987) for the ferryl-oxo complexes of imidazole-ligated iron octaethylporphyrin (OEP), protoporphyrin IX dimethyl ester (PPDME), and tetraphenylporphyrin (TPP). Furthermore, the lack of an H_2O/D_2O exchange effect indicates that hydrogen bonding to the $Fe^{IV}=O$ moiety is weak or absent and that the ferryl intermediate is relatively unperturbed by interactions with nearby amino-acid residues or ligands bound to Cu_B. Decay of the ferryl-oxo intermediate may reflect formation of a μ-oxo $a_3^{3+}Cu_B^{2+}$ adduct or of a cytochrome a_3-hydroxide intermediate upon reduction and protonation. Such intermediates have been postulated by Wikstrom(1981), Blair et al., 1983; and Chan et al.(1988). More recently, Han et al.(1989), by photoreducing the resting enzyme under intense laser illumination, observed a mode at 477 cm^{-1} that they

TABLE I

Vibrational frequencies for ferryl oxy complexes[a]

Species	$\nu(Fe^{IV}=O)$	References
Cytochrome oxidase ($a_3^{4+}=O$)	790	this work
$Fe^{IV}=O$ (TPP)	852	Proniewicz et al. (1986) Bajdor et al. (1989)
(NMI) $Fe^{IV}=O$ (PPDME)	820	Kean et al. (1987) Oertling et al. (1990)
(NMI) $Fe^{IV}=O$ (OEP)	820	Kean et al. (1987) Oertling et al. (1990)
(NMI) $Fe^{IV}=O$ (TPP)	820	Kean et al. (1987) Oertling et al. (1990)
(NMI) $Fe^{IV}=O$ ($T_{piv}PP$)	807	Schappacher et al. (1986)
(THF) $Fe^{IV}=O$ ($T_{piv}PP$)	829	Schappacher et al. (1986)
Mb $Fe^{IV}=O$, (pH 8.5)	797	Sitter et al. (1985a)
HRP-II (pH 7)	775	Terner et al. (1985) Hashimoto et al. (1986)
HRP-II (pH 11)	787	Hashimoto et al. (1984) Sitter et al. (1985b)
MPO-II (pH 11)	782	Oertling et al. (1988)
LPO-II (pH 6-10)	745	Reczek et al. (1990)

[a] Abbreviations: (TPP), meso-tetraphenylporphyrin; $T_{piv}PP$, tetra-(O-piraloylphenyl) porphyrin; PPDME, protoporphyrin IX dimethyl ester; NMI, 1-methyl imidazole; OEP, octaethylporphyrin; Mb, myoglobin; HRP-II, horseradish peroxidase compound II; MPO-II, myeloperoxidase compound II; LPO-II, lactoperoxidase compound II.

assigned to the Fe^{3+}-OH intermediate. Its role in the catalytic function of cytochrome c oxidase under physiological conditions, however, was not established.

Combining the results above with the earlier optical, EPR, and Raman results on the reduction of dioxygen by fully-reduced cytochrome oxidase, the following points emerge. First, oxygen binding occurs rapidly to form oxycytochrome a_3 and is followed by one electron intramolecular transfer from the cytochrome a/Cu_A centers to form a three electron-reduced binuclear site within 100 μs. The nature of the bound oxygen intermediates following the oxy species remains to be determined. Second, the oxidation of a and Cu_A follows a branched pathway and is biphasic under most experimental conditions that have been used. The slower phase of oxidation occurs in the 500-1000 μs time range and produces a four electron-reduced a_3/Cu_B/oxygen center. Third, in the four electron-reduced species, a ferryl intermediate that may be formulated as $a_3^{4+}=O/Cu_B^{1+}$ accumulates. Subsequent redox and ligand rearrangement produces the oxidized enzyme.

FUTURE WORK

At the present time, it is not possible to address conclusively the structure of the three-electron reduced enzyme/O_2 adduct and, therefore, the catalytic pathway(s) in the reduction of oxygen by cytochrome oxidase. In addition to the work presented here, I have recorded time-resolved

resonance Raman spectra in the 650-950 cm^{-1} region, which suggest that an oxygen isotope sensitive transient species is detected in this region at intermediate times. The 100 μs spectrum shows a vibrational mode at 865 cm^{-1}, which appears to shift to 835 cm^{-1} when the 100 μs experiment is repeated with $^{18}O_2$. The 865 cm^{-1} mode is absent in the 10 ns and 10 μs spectra, the latter of which is important because the 571 cm^{-1} a_3^{2+}-O_2 complex has scattering intensity at 10 μs. The 865 cm^{-1} intermediate is also absent in the 300 μs spectrum, indicating that it has converted to later intermediates at this time. These results suggest a number of experiments. First, we intend to repeat these experiments with mixed $^{16}O/^{18}O$ isotopes. This will allow us to determine whether the vibrator contains one or two oxygen atoms. Second, branching in the reduction reaction must be considered. Hill and Greenwood have used such a model to rationalize room temperature optical data. Monitoring the time evolution of the three-electron enzyme/O_2 species as a function of pH, and with D_2O as a solvent, will provide the opportunity to explore the dioxygen reduction and proton-translocation mechanism in detail.

REFERENCES

Argade, P. V.; Ching, Y.-C.; and Rousseau, D. L. (1986), Biophys. J. **50**, 613-620.

Babcock, G. T. (1988), "Biological Applications of Raman Scattering" (Spiro, T. G., ed.), Vol. 3, 295-346.

Babcock, G. T.; Callahan, P. M.; Ondrias, M. R.; and Salmeen, I. (1981), Biochemistry **20**, 959-966.

Babcock, G. T.; Jean, J. M.; Johnston, L. N.; Palmer, G.; and Woodruff, W. H. (1984), J. Am. Chem. Soc. **106**, 8305-8306.

Babcock, G. T.; Jean, J. M.; Johnston, L. N.; Woodruff, W. H.; and Palmer, G. (1985), J. Inorg. Biochem. **23**, 243-251.

Bajdor, K. and Nakamoto, K. (1989), J. Am. Chem. Soc. **106**, 3045-3046.

Blair, D. F.; Martin, C. T.; Gelles, J.; Wang, H.; Brudvig, G. W.; Stevens, T. H.; and Chan, S. I. (1983) Chemica Scripta **21**, 43-53.

Blair, D. F.; Witt, S. N.; and Chan, S. I. (1985), J. Am. Chem. Soc. **107**, 7389-7399.

Brunori, M. and Gibson, Q. N. (1983), EMBO J. **2**, 2025-2026.

Carter, K. R.; Antalis, T. M.; Palmer, G. M.; Ferris, N. S.; and Woodruff, W. H. (1981), Proc. Natl. Acad. Sci. U. S. A. **78**, 1652-1655.

Chan, S. I.; Witt, S. N.; and Blair, D. F. (1988), Chemica Scripta **28A**, 51-56.

Chance, B.; Saronio, C.; and Leigh, J. S. (1975a), J. Biol. Chem. **250**, 9226-9237.

Chance, B.; Saronio, C.; and Leigh, J. S. (1975b), Proc. Natl. Acad. Sci. U. S. A. **72**, 1635-1640.

Ching, Y.-C.; Argade, P. V.; and Rousseau, D. L. (1985), Biochemistry **24**, 4938-4946.

Clore, G. M.; Andreasson, L. E.; Karlsson, B.; Aasa, R.; and Malmstrom, B. G. (1980), Biochem. J. **185**, 139-154.

Findsen, E. W.; Centeno, J.; Babcock, G. T.; and Ondrias, M. R. (1987), J. Am. Chem. Soc. **109**, 5367-5372.

Gibson, Q. and Greenwood, C. (1963), Biochem. J. **86**, 541-554.

Greenwood, C. and Gibson, Q. (1967), J. Biol. Chem. **242**, 1781-1787.

Han, S.; Ching, Y.-C.; and Rousseau, D. L. (1989), J. Biol. Chem. **264**, 6604-6607.

Han, S.; Ching, Y.-C.; and Rousseau, D. L. (1990a), Biochemistry **29**, 1380-1384.

Han, S.; Ching, Y.-C.; and Rousseau, D. L. (1990b), Proc. Natl. Acad. Sci. U. S. A. **87**, 2491-2495.

Hartzell, R. and Beinert, H. (1974), Biochim. Biophys. Acta **368**, 318-338.

Hashimoto, S.; Tatsuno, V.; and Kitagawa, T. (1984), Proc. J. Ph. Acad. Ser. B **60**, 345-348.

Hashimoto, S.; Tatsuno, Y.; and Kitagawa, T. (1986) Proc. Natl. Acad. Sci. U. S. A. **83**, 2417-2421.

Hill, B. C. and Greenwood, C. (1983), Biochem. J. **215**, 659-667.

Hill, B. and Greenwood, C. (1984), Biochem. J. **218**, 913-921.

Hill, B.; Greenwood C.; and Nichols, P. (1986), Biochim. Biophys. Acta **853**, 91-113.

Kean, R. T.; Oertling, W. A.; and Babcock, G. T. (1987), J. Am. Chem. Soc. **109**, 2185-2187.

Oertling, W. A. and Babcock, G. T. (1988), Biochemistry **27**, 3331-3338.

Oertling, W. A.; Hoogland, H.; Babcock, G. T.; and Wever, R. (1988), Biochemistry **27**, 5395-5400.

Oertling, W. A.; Kean, R. T.; Wever, R.; and Babcock, G. T. (1990), Inorg. Chem., in press.

Ogura, T.; Yoshikawa, S.; and Kitagawa, T. (1985), Biochim. Biophys. Acta **832**, 220-223.

Ogura, T.; Yoshikawa, S.; and Kitagawa, T. (1989), Biochemistry **28**, 8022-8027.

Ogura, T.; Yoshikawa, S.; and Kitagawa, T. (1990), submitted.

Oliveberg, M.; Brzezinski, P.; and Malmstrom, B. G. (1990), Biochim. Biophys. Acta **977**, 322-328.

Orii, Y. (1984), J. Biol. Chem. **259**, 7187-7190.

Orii, Y. (1988), Annals of the New York Academy of Science **550**, 105-117.

Proniewicz, L. M.; Bajdor, K.; and Nakamoto, K. J. (1986), J. Phys. Chem. **90**, 1760-1766.

Reczek, C. M.; Sitter, A. J.; and Terner J. (1990), J. Mol. Struc., in press.

Schappacher, M.; Chettard, G.; and Weiss, R. J. (1986), J. Chem. Soc. Chem. Comm. **2**, 93-94.

Sitter, A. J.; Reczek, C. M.; and Terner, J. (1985a), Biochem. Biophys. Acta **828**, 229-235.

Sitter, A. J.; Reczek, C. M.; and Terner, J. (1985b), J. Biol. Chem. **260**, 7515-7522.

Terner, J.; Sitter, A. J.; and Reczek, C. M. (1985), Biochem. Biophys. Acta **828**, 73-80.

Varotsis, C.; Woodruff, W. H.; and Babcock, G. T. (1989), J. Am. Chem. Soc. **111**, 6439-6440; (1990) **112**, 1297.

Varotsis, C.; Woodruff, W. H.; and Babcock, G. T. (1990a), J. Biol. Chem., in press

Varotsis, C.; Oertling, W. A.; and Babcock, G. T. (1990b), App. Spectroscopy, in press.

Vanneste, W. H. (1966), Biochemistry **5**, 838-847.

Wikstrom, M. (1981), Proc. Natl. Acad. Sci. U. S. A. **78**, 4051-4053.

Wikstrom, M. (1989), Nature **338**, 776-778.

Wikstrom, M.; Krab, K.; and Saraste, M. (1981), "Cytochrome Oxidase, a Synthesis", Acad. Press, New York.

Woodruff, W. H.; Dallinger, R. F.; Antalis, T. M.; and

Palmer, G. (1981), Biochemistry **20**, 1332-1338.